

Journal of Materials Chemistry A

Accepted Manuscript



This is an *Accepted Manuscript*, which has been through the Royal Society of Chemistry peer review process and has been accepted for publication.

Accepted Manuscripts are published online shortly after acceptance, before technical editing, formatting and proof reading. Using this free service, authors can make their results available to the community, in citable form, before we publish the edited article. We will replace this *Accepted Manuscript* with the edited and formatted *Advance Article* as soon as it is available.

You can find more information about *Accepted Manuscripts* in the [Information for Authors](#).

Please note that technical editing may introduce minor changes to the text and/or graphics, which may alter content. The journal's standard [Terms & Conditions](#) and the [Ethical guidelines](#) still apply. In no event shall the Royal Society of Chemistry be held responsible for any errors or omissions in this *Accepted Manuscript* or any consequences arising from the use of any information it contains.



www.rsc.org/materialsA

1 11 Nov. 2015 R 2

2 **Metal organic frameworks for the control and management of air quality:**
3 **Advances and future direction**

4
5 Pawan Kumar¹, Ki-Hyun Kim^{1,*}, Eilhann E. Kwon², Jan Szulejko¹

6 ¹Dept. of Civil & Environmental Engineering, Hanyang University, 222 Wangsimni-Ro, Seoul 133-791,
7 Republic of Korea,

8 ²Department of Environment and Energy, Sejong University, Seoul 143-747, Republic of Korea

9 *E-mail: kkim61@hanyang.ac.kr, Tel.: +82 2220 2325; Fax: +82 2 2220 1945

10 **Abstract**

11 Recently, the potential role of metal organic framework (MOFs) and porous coordination polymers
12 (PCPs) has been recognized in the field of air quality management (AQM) due to their intrinsically
13 tunable chemical structure and multifunctional properties which afforded significant enhancements in
14 adsorption capacities, catalytic degradation, and removal of diverse airborne pollutants and other
15 vapors. A diverse range of MOFs was investigated for separation, capture, and storage of greenhouse
16 gases and other pollutants (including volatile organic compounds (VOCs), sulfur compounds, and
17 chemical warfare agents (CWAs)). Also, we discuss their main drawbacks such as poor selectivity,
18 high energy and fiscal cost, low capacity, and difficulties in regeneration. Here, we provide an up-to-
19 date review on the promising role of MOFs in the field of AQM in relation to the diverse available
20 synthesis methods. As such, we hope to provide a meaningful direction for success in our efforts on
21 air quality control that MOFs/PCPs can offer for a bright future.

22
23 **Keywords:** Metal organic frameworks, toxic gases and chemicals, adsorption, removal

24 Introduction

25 A wide array of anthropogenic hazardous pollutants including NO_x, SO_x, CO, H₂S, NH₃,
26 hydrogen cyanide, volatile organic compounds (VOCs), and polycyclic aromatic compounds
27 (PAHs) are released from both static and mobile sources (e.g., industrial, transport, household,
28 fossil fuels use, and many other sources). They are emitted into the atmosphere, taken up by
29 plants, and ingested by animals to be bio accumulated along the food chain up to the apex
30 predator. Most of these pollutants are classified as being toxic/carcinogenic by varying degrees
31 and pose a worldwide risk to the environment and human health.¹⁻⁴

32 Exposure (through different exposure pathways i.e., inhalation, dermal absorption, ingestion,
33 and etc.) to those hazardous pollutants can damage the immune, neurological, reproductive (e.g.,
34 reduced fertility), developmental, and respiratory systems of humans and animals.⁴⁻⁷ As
35 summarized in recent articles, the toxicity levels of hazardous pollutants are established by
36 different agencies on the basis of their metabolic impacts and physico-chemical properties.⁸⁻⁹ In
37 summary, clean air is one of the most daunting challenges to improve the quality for life on
38 Earth.

39 For more eco-friendlier and economical air quality management (AQM), much research has
40 been done over the last 60 years.⁸⁻⁹ More recently, the practical applications of porous metal
41 organic framework (MOFs)/porous coordination polymers (PCPs) is being recognized for AQM
42 because of their potential versatility, especially in the capture and/or adsorption, the enhanced
43 catalytic effects on air-borne pollutants (due to high selectivity, chemical and thermal stability in
44 the low and mid temperature range, moderate/low heat of adsorption, and enhanced mass uptake
45 (e.g., through modification of the pore size).⁸⁻¹⁷ Thus, MOFs/PCPs are recognized as alternative
46 sorbent or catalytic media to replace or support conventional materials (such as charcoal,
47 activated carbon, alum inosilicates, and zeolites) for adsorbent and catalytic degradation
48 applications (**Figure 1**).¹²

49 Basically, a framework of coordinately bound metal ions with organic linkers can offer flexible
50 chemical properties, extremely low framework density ($0.2\text{--}0.6\text{ g.cm}^{-3}$), wide range of tunable
51 pore sizes, and specific high surface areas with quasi-infinite selection of crystal structure.¹⁸⁻¹⁹
52 More interestingly, various options for synthetic methods (solvothermal, hydrothermal,
53 microprecipitation, layer by layer, etc.) for PCPs or MOFs facilitate the expansion of their
54 applicabilities. For instance, MOF-5, MOF-177, and MOF-199 have demonstrated unique
55 optical, electrochemical, and electromechanical properties to trap guest species.²⁰⁻²³ Additionally,
56 improvement in modification of rigid MOFs chemical structure (modified functionalized MOFs,
57 isorecticular metal organic frameworks (IRMOFs), multivariate metal organic framework
58 (MVTMOFs), etc.) allows to enhance chemical flexibility with reversible variable pore sizes
59 (and volumes) to simulate a ‘breathing effect’.¹⁸⁻²³ Furthermore, excellent catalytic property at
60 the low and mid temperature ranges was regarded as the ideal goal of air purification treatment
61 to produce low-risk secondary emissions to some extent; it should thus allow to overcome many
62 limitations encountered in sorptive approaches, e.g., secondary emission of captured pollutants
63 after saturation.²⁴⁻²⁵ If one enables fine tuning of the catalytic properties of MOFs, then it
64 possibly degrade toxic substances into nontoxic products. However, as there are only a limited
65 number of reports detailing such processes, it is desirable to establish future scientific
66 benchmarks that can be directly applicable to AQM.

67 Many advances in (human) lifestyle quality have been achieved through the improvements in
68 air quality and its protection. A number of review articles and monographs have been reported to
69 describe the fundamental science of MOFs on the applications of adsorptive and catalytic
70 treatment of pollutants.¹⁸⁻²⁸ In this review; we discuss the synthesis methods of MOF/PCP to
71 account for their application toward the adsorption and catalytic degradation of airborne
72 pollutants. To this end, the underlying capacity of MOFs has been evaluated in viewpoint of their
73 potent role in the technological advancement of AQM. The state of art performance of MOFs in

74 AQM is hence described by emphasizing a number of case studies made in field applications.
75 The scope of this review will be extended further to address the future opportunities to furnish a
76 desirable roadmap for their applications to AQM.

77

78 **Current strategy for MOFs in AQM**

79 The excellent identified features of MOFs for AQM applications can be achieved or
80 maximized with the aid of effective strategies in their synthesis. For their synthesis, the
81 combination of several variables like the choice of metal ions, organic linkers, solvents,
82 synthetic/post synthetic methods, and experimental conditions is important.²⁹⁻³⁰ In addition,
83 improved performance of MOFs have also been reported by modifying their structures (e.g.,
84 functionalization, pre-functionalization of organic linkers, mixed organic linkers, mixing of
85 different metal nodes, thin film coating, hybrid textiles, and shell adsorbent).²⁹⁻³⁶ For instance,
86 one target can be retained strongly in preference to others through particular surface chemistry
87 offer by MOFs. Likewise, adsorption selectivity can easily enhanced through change in the
88 structural properties towards coordination bonding, acid–base/electrostatic interactions, π -
89 complex/H-bonding formation, open metal sites on the pore surface in MOFs.³⁷⁻⁴⁰

90 In terms of cost-effectiveness, the synthesis cost of MOF/PCP is much high relative to
91 commercialized/conventional agents for AQM. As such, it becomes major question as to their
92 practical applications on a megascale. For instance, if CO₂ is adsorbed and desorbed by MOFs
93 using a temperature–swing adsorption (TSA) approach, then both energy and financial cost are
94 expected to be very uncompetitive compared to existing sorbents. According to a survey, the free
95 on board (FOB) commodity prices (in USD) for two of the mostly studied MOFs (MOF-5 and
96 MOF-177) are \$200/kg and \$130k/kg, respectively which are highly more expensive in
97 comparison to more conventional sorbent materials (such as monoethanolamine (\$2.66/kg) and

98 quicklime (\$0.18).⁴¹⁻⁴² In the case of MOF-TSA, the energy cost is high due to high parasitic
99 energy consumption and in addition, the MOF material costs are extremely high. Thus, for an
100 example, if two columns of MOFs are working 14 hours per cycle for capturing CO₂ using a
101 parasitic 220 megawatt (MW) power load from 500 MW coal-fired power plant, the actual cost
102 for CO₂ capture and storage using MOF/PCP would be \$0.66 M per day.⁴¹⁻⁴² In comparison, a
103 conventional and well established material like that MEA, would be \$0.26 per kg for CO₂
104 capture and storage. Hence, MOF/PCP has currently a low appeal for future industrial
105 applications for CO₂ capture based on material and infrastructure costs. Therefore, an effective
106 and low cost MOF synthesis strategy is a primary requirement for any industrial application.
107 However, some excellent performance features (e.g., chemical tunability, high adsorption
108 capacity, and adsorption selectivity) of MOF/PCP can partly offset the high material costs and
109 thus play an increasingly promising role for AQM in the near future.

110 In addition, separation and regeneration of MOFs for the purpose of heterogeneous catalyst
111 has been considered one of the most attractive research areas for AQM. The catalytic activity of
112 MOFs has yet fully been investigated for the removal of toxic airborne gaseous chemicals.^{8-9, 43-}
113 ⁴⁴ Basically, as the catalytic activity is highly contingent on MOF/PCP's crystal lattice structure,
114 specific synthetic strategies for the selection and arrangement of basic building blocks (metal or
115 organic linkers) with desired chemical structure and properties could be expected. Interestingly,
116 heterogeneous catalysts in MOFs were thought to occur by host-guest mechanism through
117 transition state recognition, regulation of luminescence, and allosteric nature enforced by their
118 physical, chemical, and environmental stimuli response.⁴⁵⁻⁴⁶ Nonetheless, a number of issues
119 (waste disposal and high cost) still remain as the major drawbacks in the heterogeneous catalysts
120 of porous materials. Therefore, there is a crucial need for functional engineering of MOF/PCP to

121 attain excellent and specific catalysis properties with their advantageous physicochemical
122 properties for their future practical utilizations.

123

124 **MOFs as media for adsorptive removal of air pollutants**

125 Among various AQM control techniques, the use of sorbents have been most developed and
126 employed as an effective option to treat or remove toxic air pollutants. Various commercialized
127 sorbent materials (e.g., activated carbon, zeolites, polymers, activated alumina, silica gel, etc.)
128 have been evaluated and utilized for storage, separation, purification, and removal of pollutants
129 in industry (**Table 1**).⁴⁷⁻⁵⁹ However, these existing conventional sorbents may not fully meet the
130 high quality standard required for the future technological demands in terms of environmental
131 regulations (e.g., disposal of spent sorbents) and more stringent “greener” energy requirements.
132 This section will therefore focus on these issues and present an up-to-date appraisal and
133 information on the various and numerous MOFs reported in the literature.

134

135 **Fundamental aspect and mechanism of adsorptive removal by MOF/PCP**

136 The unique permanent porous structure of MOFs (in air) has been recognized and led to
137 practical AQM applications.⁶⁰⁻⁶¹ The PCPs/MOF adsorption properties depend on well-known
138 factors: 1] solute hydrophobicity, 2] sorbent surface area and porosity, and 3] organic carbon
139 content and mineral composition.⁶¹⁻⁶³ In addition, fundamental mechanism for selective
140 adsorption is favored by various adsorption mechanisms (such as electrostatic interaction, acid-
141 base interaction, hydrogen bonding, π — π stacking/interaction, and hydrophobic interaction) for
142 AQM (**Figure 2**).⁶³ These different MOF mechanism classes have also been described for
143 hazardous organics from aqueous media.⁶³ This well organized review was helpful to explain
144 selective adsorption mechanism with respect to MOFs. In this review, we are mainly focusing to

145 describe the fundamental aspects of these diverse mechanisms for the selective adsorption
146 processes mainly to deal with various airborne species.

147 Adsorption isotherms have generally been interpreted by well-known theories developed by
148 Freundlich, Langmuir, and Brunauer–Emmett–Teller (BET).⁸⁻⁹ Basically, an adsorption isotherm
149 is the plot of adsorbate mass on the surface of adsorbent as function of adsorbate partial pressure
150 at constant temperature. The recommended definitions and characteristics of adsorption isotherm
151 hysteresis have been discussed in an IUPAC report (1985) with an update is scheduled in 2015 to
152 classify the effect of important variables (e.g., pore size, isotherm type, and hysteresis loops).⁶³
153 In this review, we have followed the definition of the adsorption isotherm and hysteresis given in
154 the older IUPAC report (1985).⁶⁴ **Figure 3** illustrates the classification of different fundamental
155 isotherms and hysteresis types.^{60,64} For the sorptive removal by MOFs, adsorption isotherm can
156 provide the direct information regarding their hydrophilic and hydrophobic nature. In some
157 mesoporous materials, hysteresis loops are always close and adsorbate remains in the pores even
158 at near zero pressure. In such materials, high temperature should either lead to desorption or
159 irreversible adsorption in pores the same size of the adsorbate molecules.^{8,66} The adsorption
160 processes in MOFs can proceed according to their chemical nature and structure stability in
161 aqueous or non-aqueous phase with isotherm type I (microporous MOFs with strong adsorbate-
162 adsorbent interactions), III (an unusual hybrid with a larger pore size), and IV (mesoporous
163 MOFs with ≥ 20 Å diameter pore size).⁵⁹ Note that type II isotherms have been investigated for
164 unrestricted monolayer-multilayer adsorption from non-porous or macroporous materials.⁶⁶
165 However, there should be very different adsorption mechanisms between different MOFs, e.g.,
166 MOF-53 due to its flexible chemical nature and stability.⁶⁵⁻⁶⁶

167

168 **MOFs for the removal/storage of greenhouse gas (GHG): CO₂**

169 In last few years, a large number of MOFs were investigated to generate extensive
170 experimental data on the strategic adsorption of pollutants for industrial applications. The
171 adsorption, storage, and removal of CO₂ under standard temperature pressure (STP) conditions
172 have been reported for more than 130 MOFs (e.g., Cu-BTtri, CPO-27, HKUST-1, bio-MOF-11,
173 MIL-53, MOF-5, MIL-100, MIL-101, and YO-MOF).⁶⁷⁻⁷¹ The performance or capacity of CO₂
174 capturing by MOFs can be classified by the following criteria: open metal sites, flexible
175 chemical structure, and functionalization.⁶⁹ Likewise, the combination of open metal sites and H-
176 bonding donor-acceptor groups in MOFs should contribute to the efficient removal of other
177 gaseous pollutants as well. Functionalization or surface modification of MOFs (e.g., with
178 ethylene diamine and other alkyl amines) has been investigated to seek for the extension of their
179 applications in a more broad areas (as per discuss in Section 2).

180 In this section, the adsorption capacity of the modified/functionalized MOFs is explored for
181 low molecular weight gases at low pressure with a special emphasis on CO₂ (**Table 2**).⁷²⁻⁸² For
182 examples, Britt et al.⁷² investigated open magnesium sites based Mg-MOF-74 for the
183 CO₂ capture with 8.9 wt% dynamic capacity which underwent facile CO₂ release at significantly
184 lower temperature (80 °C). These results were obtained at ambient atmosphere and regeneration
185 of Mg-MOF-74 was also demonstrated on the breakthrough apparatus under N₂ atmosphere at
186 least 250 °C before use.⁷² Recently, a highly robust unprecedented anionic MOF (JUC-132)
187 based on an aromatic 12-carboxyl ligand 1,3,5-tris(3,5-di(3,5-dicarboxy-phenyl-1-yl)-phenyl-1-
188 yl)benzene (H₁₂TDDPB) and two Cd clusters (Cd₂(COO)₆ and Cd(COO)₄) synthesis was
189 investigated for selective adsorption of CO₂ over CH₄.⁷³ JUC-132 exhibited high heat of
190 adsorption for CO₂ with high selectivity over CH₄ due to high interactions between CO₂ and
191 filling of dimethylammonium ions in the pores. He et al.⁷³ reported uptake values of activated
192 JUC-132 for CO₂ (2.72 mmol g⁻¹ and 1.71 mmol g⁻¹ at 1 atm) and CH₄ (0.28 mmol g⁻¹ at 1 atm)
193 at different temperatures (273K and 278K, respectively).

194 To enhance the adsorption capacity of CO₂, the capacity of several virgin (and some
195 modified/functionalized) MOFs is compared in **Table 2**.⁷²⁻⁸² A simple modification or
196 functionalization of Mg(DOBDC) MOF was carried out with ethylene diamine (ED) to improve
197 the adsorption properties of CO₂ at low partial pressures.⁷⁶ Based on theoretical and
198 experimental analysis, these authors confirmed that one ED molecule was added to each unit cell
199 of Mg(DOBDC) MOF. This modification allowed improved CO₂ adsorption-desorption
200 temperature swings (give both low and hi temps) with increased CO₂ adsorption capacity at
201 ultra-low CO₂ partial pressures at 1 atm total pressure together with improved Mg(DOBDC)
202 MOF regenerability over 20 swings. According to this report, the first MOF was demonstrated to
203 yield significant adsorption capacities from simulated ambient air (e.g., 400 ppm CO₂ at 1 bar
204 pressure) compared to the common conventional adsorbents (e.g., amine-oxide composites).⁷⁶
205 Similarly, diamine-functionalized en-Mg₂(dobpdc) was achieved through post modification to
206 yield the exceptionally high sorption capacities (e.g., 3.62 mmol g⁻¹, 13.7 wt% for both ambient
207 air (4.0x10⁻⁴ bar of CO₂) and typical post-combustion flue gas (0.15 bar of CO₂) at 1 bar.⁷⁶ The
208 adsorption of CO₂ onto the free amines of MOF/PCP led to the formation of carbamic acid
209 which significantly increased the CO₂ adsorption capacity. Finally, to facilitate the practical
210 utilization of MOF, the adsorption-desorption cycling of CO₂ was optimized at the real dilute
211 concentrations of air and flue gas.⁷⁶

212 A pioneering work on the unprecedented mechanism of step-shaped isotherms was carried out
213 by McDonald et al. (2015).⁸⁰ Their study demonstrated that the replacement of Mg²⁺ with other
214 divalent metal ions (e.g., Mn²⁺, Fe²⁺, Co²⁺, and Zn²⁺) can tailor the CO₂ adsorption isotherm
215 steps depending on the metal-amine bond strength. Here, the diamine-appended MOF/PCP
216 behaved as ‘phase-change’ adsorbents to facilitate the efficient capture of CO₂.⁸⁰ The CO₂
217 adsorption was thus improved via thermodynamically non-spontaneous reaction at low pressure
218 which had been demonstrated by spectroscopic, X-ray diffraction, and adsorption analysis.

219 Actually, the proton transfer and nucleophilic attack of N proceeded simultaneously on a CO₂
220 molecule to form ammonium carbamate. The amine coordination at the next metal site was then
221 destabilized by diamine-appended MOF/PCP to initiate the cooperative adsorption of CO₂ by a
222 chain reaction (**Figure 4**).⁸⁰

223

224 **MOFs for the removal/storage of common gases and hazardous air pollutants (HAPs)**

225 The utilization of MOFs for low molecular weight gases other than CO₂ has also been studied
226 extensively for their storage potential (e.g., for H₂ and CH₄ as alternative vehicle fuels).⁸³⁻⁹⁶

227 Other adsorbent media for low molecular weight gasses (such as H₂, CH₄, N₂O, and N₂) using
228 various approaches have been tested. In this respect, Eddaoudi et al. (2001) reported a
229 remarkable improvement in CH₄ storage capacity by series of isorecticular MOFs (IRMOFs).⁸⁴

230 Likewise, IRMOFs-6 with exceptionally high surface area and pore volumes was also tested for
231 sorption measurement (10 mmol(CH₄).g⁻¹ at 40 atm but at lower pressures, e.g., 1 atm, the
232 sorption is only ~0.4 mmol (CH₄).g⁻¹ implying good PSA performance at constant temperature
233 (**Figure 5 A & B**).⁸⁴ In an analogous way, Duren et al. (2004) evaluated storage capacity of CH₄

234 based on molecular modeling of IRMOFs, two zeolites, MCM-41, and carbon nanotubes.⁸⁵

235 Accordingly, the amount of adsorbed CH₄ per volume increased by 23% and 36%, when 1,4-
236 tetrabromobenzenedicarboxylate and 9,10-anthracenedicarboxylate were used as organic linkers,

237 respectively. Their experimental study underlined the usefulness of grand canonical Monte Carlo
238 (GCMC) simulations method as a screening tool to identify new materials for adsorption

239 applications and for the design of novel materials. For hydrogen adsorption studies, similar
240 approaches were also investigated.⁸⁶⁻⁸⁷ Furthermore, GCMC simulation results demonstrated that

241 chemical structural properties in MOFs with unsaturated metal centers can be incorporated to
242 increase the magnitude of hydrogen interaction within their framework.⁹⁰ Such molecular

243 modelling method was also utilized to determine the adsorption of ammonia for a number of
244 MOFs (MIL-47, IRMOF-10, IRMOF-1, IRMOF-16).⁸⁷

245 It is found that the selection of different functional groups (e.g., -OH, -NH₂, -COOH and
246 metal ions (Cu⁺⁺, Ag⁺, Na⁺ or K⁺) can be made to enhance chemisorption hydrogen-bonding
247 between MOFs and ammonia for improved adsorbate removal.⁸⁸⁻⁹⁶ For example, Britt et al.
248 (2008) investigated NH₃ adsorption and dynamic breakthrough using -NH₂ functionalized
249 MOFs (IRMOF-3).⁹¹ The adsorption capacity of IRMOF-3 was found as 6.2 mmol g⁻¹ which
250 was superior to the most commonly studied MOF-5 (0.35 mmol g⁻¹) as a reference. It may be
251 due to the presence of Zn₄O SBUs in MOF-5 which becomes unstable when exposed to
252 ammonia. However, in the case of IRMOF-3, the capacity of ammonia adsorption increased
253 due to hydrogen bonding between the -NH₂ pendant groups and ammonia.⁹⁰⁻⁹² In another
254 study, -OH functionalization of DUT-6 was found to improve the uptake of ammonia from
255 12.0 to 16.4 mmol g⁻¹ at 1 bar and 298 K (**Figure 6 A & B**).⁹³ Such enhancement in sorption
256 capacity was accounted for by strong binding between ammonia and functional groups (-OH).
257 ⁹³

258 For the removal of ammonia from air, a number of Zr-based MOFs (UiO-66 (UiO-66-OH,
259 UiO-66-(OH)₂, UiO-66-NO₂, UiO-66-NH₂, UiO-66-SO₃H, and UiO-66-(COOH)₂) were also
260 investigated.⁹⁴ Comparison of performance was made between those Zr-based functionalized
261 MOFs synthesized by solvothermal method. Accordingly, different functional groups such as (-
262 OH, -NO₂, -NH₂, -SO₃H, and -COOH) played an important role in ammonia adsorption
263 processes under dry and humid (80% RH) conditions due to competitive interactions between
264 water and ammonia molecules for the active sites. Interestingly, -COOH and -SO₃H based
265 functionalization of Zr-MOFs showed lower ammonia capacity as compared to -OH and NH₂
266 (UiO-66-OH and UiO-66-NH₂) due to the presence of high and least bulky functional groups
267 which caused significant reduction in the framework porosity (surface area and pore volume),

268 respectively. Finally, the adsorption capacity of ammonia by UiO-66-OH was reported as
269 ~ 5.7 mmol/g under dry conditions.⁹⁴ The GCMC simulations were also carried out for the
270 practical applications of pressure swing adsorption (PSA) using a MIL-53 (Al).⁹⁴ These authors
271 investigated the feasibility of MOFs for methane purification at industrial-scale. The adsorption
272 capacity of MIL-53 (Al) (4.3 mol.kg^{-1} at 3.5 bar) was assessed against CO_2 and CH_4 by dynamic
273 experiments in a fixed-bed reactor and 303 K). As MIL-53(Al)-based separation is found to be
274 highly energy-efficient, the proposed PSA was suggested as a promising option for the
275 separation of CO_2 and CH_4 .⁹⁴

276 MOFs have also been identified as attractive sorbent candidates for PSA separation of O_2 .
277 Many research groups investigated the O_2 selectivity against H_2 , CO_2 , or N_2 based on the
278 tunability of MOFs with unsaturated metal centers (UMCs).⁹¹⁻⁹⁹ For example, the selectivity of
279 O_2 over N_2 was examined through utilization of two different MOFs ($\text{Cr}_2(\text{BTC})_3$ vs.
280 $\text{Fe}_2(\text{DOBDC})$) prototypical phases that have accessibility to UMCs for single gas sorption
281 studies at 298 K.⁹⁷ Likewise, the combination of experimental and molecular modeling was
282 tested more recently using metal-substituted Cu-BTC (HKUST-1) with enhanced O_2 selectivity
283 versus N_2 .⁹⁷ Here, the structure-property relationship was examined between the metal centers
284 and the gas adsorption (O_2 or N_2) at variable temperatures (77 K vs. 273–298 K) (**Figure 7 A &**
285 **B**).⁹⁷ A comparative analysis was also made for O_2 versus N_2 sorption capacities and binding
286 energy dependency on temperature based on density functional theory (DFT) calculations and
287 GCMC.⁹⁷ Moreover, MOFs have also been studied for purification and storage of C_1 , C_2 , and C_3
288 light hydrocarbons.⁹⁸⁻⁹⁹ As part of such efforts, Fu et al. (2015) recently reported the FIR-51
289 (CPs/MOF) for selective sorption of light hydrocarbons (**Figure 8 A & B**).⁹⁹ The synthesized
290 MOF/PCP was highly stable (thermally and chemically) to exhibit high storage capacity ($3.12 -$
291 7.06 mmol g^{-1}) for light hydrocarbons with high selectivity for C_2 and C_3 over methane at 273
292 and 294 K (**Figure 8 B**).⁹⁹

293 Presently, the efficient adsorption removal of hazardous air pollutants (HAPs) is one of the most
294 attractive research areas in AQM. This section summarizes the recent efforts made on the
295 adsorptive removal of those pollutants contained in fuel, water, and air by employing advanced
296 MOFs. For the adsorptive removal of H₂S, VOCs, and PAH, the feasibility of many MOFs (such
297 as Material de Institut Lavoisier (MIL), IRMOFs, and M-CPO) has been investigated intensively
298 (**Table 2**). The interactions between HAPs and different MOFs should proceed via diverse
299 mechanisms; (a) adsorption through coordinately unsaturated site, (b) acid-base interaction, (c)
300 complex formation, (d) hydrogen bonds, (e) electrostatic interaction, and (f) lattice breathing.⁹⁹⁻
301 ¹⁰⁵

302 Recently, amino functionalized UIO-66 was reported to absorb pyridines with the hydrogen
303 bonding and base-base repulsion in both liquid and vapour phases.¹⁰¹ The possible interaction
304 between pyridine and amino functionalized UIO-66 is shown in **Figure 9 A**.¹⁰¹ The temperature
305 effect on such absorption by functionalized UIO-66 is also illustrated in **Figure 9 (B, C, and**
306 **D)**.¹⁰¹ It was concluded that the uptake rate of pyridine increased for both vapor and liquid
307 phases in line with the amino group content in UiO-66s. The specific and favorable interactions
308 between pyridine and NH₂-UIO-66 should be carefully interpreted with the opening of pores of
309 UiO-66 with increasing temperature to accommodate pyridine.⁹⁵ Likewise, a number of other
310 similar studies are shown in **Table 2**.¹⁰⁰⁻¹⁰⁵

311 In a recent study, the absorption capacity of Cu-BTC was examined against three toxic
312 hydride gases (ammonia, arsine, and hydrogen sulfide) with the changes in its color (**Figure 10**
313 **A**).¹⁰⁵ The capacity of Cu-BTC for these hydride gases was determined from a micro-
314 breakthrough test using a real-world packed-bed with both dry and at high humidity conditions
315 (**Figure 10 B**).¹⁰⁵ These authors demonstrated the potential for Cu-BTC as an effective adsorbent
316 for ammonia. They also used it for sensing purposes through colorimetric and fluorescence
317 changes. Interestingly, a recent computational study on Cu-BTC has been made to validate its

318 potential for ammonia capture in the presence of water through quantum chemical methods.¹⁰⁴⁻¹⁰⁵
319 The free energies of binding were calculated for the first time for ammonia and water separately
320 with a series of metal catecholates (i.e. Be-, Cu-, Zn-, Pt-, and Pd-catecholates). As a result, Pt-
321 and Cu-catecholates were found as the excellent choice for ammonia capturing under humid and
322 dry conditions, respectively.¹⁰¹⁻¹⁰⁵

323

324 **MOFs for catalytic degradation -Fundamental aspects and mechanism**

325 In **Table 3**, a list of MOFs employed for the catalytic degradation of airborne pollutants are
326 summarized based on the synthesis processes, active metal ions, and the basic mechanism.¹⁰⁷⁻¹¹⁴
327 As long as the precise synthesis plan is established and used, different catalytic sites can be
328 tailored in MOFs such as (A) embedding of their active sites in the cavities, (B) the use of
329 postsynthetic methods, and (C) incorporation (or encapsulation) of guest species (such as
330 functional group, metal nanoparticles, and other guest molecules) (**Figure 11**).⁴⁵

331 Recently, Al, Zn, Fe, Zr, and Cu-based MOFs have been utilized for photo-catalytic
332 applications to degrade chemicals (of varying toxicity) such as phenols, alcohols, and toxic
333 chemical warfare agents (CWA) (**Figure 12**).⁸ For example, Wang et al. first reported UiO-67
334 (Zr-MOF) heterogeneous catalyst for the photocatalytic reduction of CO₂, water oxidation, and
335 visible light-driven organic photocatalysis (**Figure 13 (A & B)**).¹⁰⁶ This doped MOF/PCP
336 behaved like efficient aerobic oxidation catalyst for thioanisole, as shown in the **Figure 13 B**.¹⁰⁶
337 Moreover, the doped MOF is convenient to reuse for heterogeneous catalysis, while effective
338 enough to provide mechanistic insights into CO₂ reduction.¹⁰⁶ Similarly, Shen et al. reported
339 efficient visible-light-driven photocatalysis for selective oxidation of alcohols with the reduction
340 of aqueous Cr(VI) using a multifunctional Zr-2-NH₂-benzenedicarboxylate (UiO-66(NH₂)).¹⁰⁷ In
341 another study, photocatalytic degradation of organic pollutants was also achieved by the
342 chemical oxidation with strong oxidative agents. Because of the transition metal species present

343 in MOFs, oxidants can be generated for the activation of free radicals. For example, MIL-53(Fe)
344 was tested for the decolorization of methylene blue (MB) dye.¹⁰⁸ MIL-53(Fe) exhibited the first-
345 order kinetics in the photocatalytic decolorization of MB.¹⁰⁸ The rate of photocatalysis decreased
346 in the order of ($\text{H}_2\text{O}_2 > (\text{NH}_4)_2\text{S}_2\text{O}_8 > \text{KBrO}_3$) under the normal UV-vis light irradiation.
347 However, under visible light irradiation, its ordering changed to $(\text{NH}_4)_2\text{S}_2\text{O}_8 > \text{H}_2\text{O}_2 > \text{KBrO}_3$.
348 Interestingly, MIL-53(Fe) showed the first-order kinetics with the rate constant (0.0133 min^{-1}
349 and 0.0036 min^{-1}) which is comparable with TiO_2 under UV-vis light and visible light
350 irradiation, respectively.¹⁰⁸

351

352 **MOFs as media for catalytic degradation of air pollutants**

353 Although a number of MOFs have been employed for catalytic treatment, there are only a few
354 reports that actually covered or described their applications toward diverse air pollutants. Many
355 excellent features of MOFs (such as controlled fine structure, dispersion of active sites, high
356 crystallinity, and no theoretical pore size limitations) have been recognized for catalytic
357 applications.¹⁰⁹⁻¹¹⁹ However, to employ these advanced materials in such aspect, one has to
358 overcome the major conventional problems such as secondary emissions after adsorbent
359 saturation.^{8-9, 109-115} Nonetheless, the versatile nature of MOFs is advantageous to use in a variety
360 of catalytic degradations. For example, Ferey et al. (2005) demonstrated the potent role of
361 nanoporous metal-organic framework (e.g., MIL-101) through immobilization of Keggin
362 heteropolytungstate within the cages of the framework.¹¹⁶ Interestingly, a rigid crystal structure
363 of MOF with large pores and outstanding surface area exhibited a great structural resistance to
364 air, water, and common solvents with thermal treatment.¹¹⁶

365 The potential role of MOFs as photocatalytic agent has been proposed for artificial
366 photosynthesis wherein gaseous CO_2 can be converted into useful products.⁹⁸⁻¹⁰³ However, as of
367 now, MOFs have not been studied intensively with that respect. For example,

368 $[\text{Re}^{\text{I}}(\text{CO})_3(\text{dcbpy})\text{Cl}]-\text{Zr}_6\text{O}_4(\text{OH})_4(\text{bpdc})$ MOF yielded carbon monoxide from CO_2 and H_2O at a
369 rate of $42 \mu\text{mol}(\text{CO})\cdot\text{h}^{-1}\cdot\text{g}^{-1}$ under 450 W Xe lamp irradiance.¹¹⁷ In a practical sense, one may
370 consider a hypothetical case in which a 500 MW power station burning coal (specific energy
371 content of $24 \text{ MJ}\cdot\text{kg}^{-1}$ and 85% carbon content) is operating at 50% thermal efficiency.¹⁰⁶⁻¹¹⁹
372 Then, the amount of CO_2 produced from such operation would correspond to $11,000 \text{ tonne}\cdot\text{day}^{-1}$.
373 Hence, in order to convert $\text{CO}_2 + 2\text{H}_2\text{O}$ into CH_4 and 2O_2 ($\Delta\text{H} = 890 \text{ kJ}\cdot\text{mol}^{-1}$ (NIST)), the area
374 of a hypothetical MOF/PCP/solar farm, operating at 100% quantum efficiency and 12-hour
375 averaged solar irradiance of $100 \text{ W}\cdot\text{m}^{-2}$, should be $\sim 52 \text{ km}^2$ (maximum CO_2 uptake is $215 \text{ g}\cdot\text{day}^{-1}$).
376 If the following conditions are taken (MOF catalyst bed = 1 mm deep, MOF density = $0.5 \text{ g}\cdot\text{m}^{-3}$,
377 and MOF cost = $2000 \text{ USD}\cdot\text{ton}^{-1}$), then the amount required and cost would be $\sim 26,300$
378 tonnes and 53 B USD, respectively. Based on this proposed hypothetical case for utilization of
379 MOF/solar farm area, conversion of CO_2 into useful products is impractical for industrial
380 applications. In other sense, this area still needs to put immense efforts to meet economic
381 feasibility.

382

383 **The use of MOF for catalytic degradation of chemical warfare**

384 MOFs have also been investigated for the catalytic degradation of chemical warfare agents
385 (CWA) due to huge environmental contamination problem after their deployment.¹⁰⁷⁻¹²¹ Usually,
386 redox or acid-base active MOFs have been used as catalyst agents for degradation processes.
387 Interestingly, CWAs can be degraded either by oxidation and as well as by hydrolysis after
388 exposure. For the interested readers, catalytic degradation mechanisms for selected CWAs can
389 be found in a study by Mondloch et al. (2015) (**Figure 14**).¹¹⁰ These authors reported both
390 experimental and computational analysis of catalytic hydrolysis of the nerve agent stimulants
391 like dimethyl 4-nitrophenyl phosphate (DMNP) and O-pinacolyl methylphosphonofluoridate
392 (Soman) using NU-1000 and NU-1000-dehyd (Zr-MOFs), respectively.¹¹⁰ In their experimental

393 study, catalytic hydrolysis of DMNP by NU-1000 was carried out efficiently in aqueous N-
394 ethylmorpholine buffered solution (at pH 10) with the formation of p-nitrophenoxide monitored
395 by visible-region adsorption spectroscopy at $E_{\max} = 407$ (**Figure 14 A & B**).¹¹⁰ In this report,
396 computational simulations have also been investigated on soman and O-ethyl S-
397 diisopropylaminoethyl methylphosphonothiolate (VX) using Cr-MOFs. Cr-MOFs was the fastest
398 heterogeneous catalyst of all tested MOFs (e.g., HKUST-1) due to the π -stacking behaviour of
399 DMNP and more general attractive van der Waals interactions between organic linker and alkyl
400 group of GD or its analog.¹¹⁰

401 Catalytic degradation of diisopropylfluorophosphate (DIFP) sarin simulant was also
402 investigated similarly using both $\text{NH}_2\text{-MIL-53(Al)}$ and $\text{NH}_2\text{-MIL-101(Al)}$ ($\text{Al-NH}_3\text{-MOF}$)
403 through the incorporation of highly nucleophilic 4-methylaminopyridine residues.¹¹⁹ This
404 progressive strategy was developed by depositing the MOF particles on a reactive adhesive
405 material composed of polyisobutylene/toluene diisocyanate (PIB/TDI) blends. These modified-
406 MOFs exhibited highly mechanical flexibility with the capability of degrading diisopropyl
407 fluorophosphates (DFP) due to their reactivity between the covalent attachment to protective
408 surfaces.¹¹³

409 The detoxification of some CWAs (e.g., VX and soman) by HKUST-1 (Cu-MOF) was
410 monitored by NMR.¹¹³ However, Cu-MOFs underwent slow degradation of these CWAs (more
411 than one day (VX) and 13 hr. (soman)) due to the Lewis acidic nature and the presence of Cu
412 open metal sites. This type of the interaction was found to be crucial in determining the
413 hydrolysis processes between Cu-MOF and CWAs.¹¹³ It was also found that the catalytic activity
414 of $\text{H}_3[(\text{Cu}_4\text{Cl})_3(\text{btc})_8]_2[\text{PW}_{12}\text{O}_{40}]_3(\text{C}_4\text{H}_{12}\text{N})_6$ (NENU-11) should be stimulated by the
415 incorporation of acid polyoxometalates in the pore structure.¹¹³ Consequently, NENU-11
416 exhibited the good sorption behavior (15.5 molecules per formula unit) for a model nerve agent
417 dimethylmethylphosphonate (DMMP) while facilitating its decomposition (**Figure 15**).¹¹³

418

419 **Summary**

420 It is found that most MOFs reported recently in the literature (2005 – 2015) have a number of
421 shortcomings for AQM applications. Most of these studies generally lacked a systematic
422 approach to evaluate practical performance metrics in some important respects, e.g., (a) low final
423 product cost and well established synthesis methods, (b) hydrothermal stability, (c) chemical
424 stability towards humidity and temperature, (d) simple regeneration at low energy penalty, and
425 (e) recycling and disposal of spent material. Because of such a research gap in this emerging
426 area, one needs a systematic evolution of MOFs for air purification to comply with international
427 guidelines (e.g., OSHA/NIOSH). Furthermore, it is very important that every investigation on
428 the MOFs for air purification be evaluated at partial pressures of environmental pollutants at
429 ambient air pressure (1 bar). However, such specific conditions for the adsorption are found to be
430 difficult to attain to cover all different permanent and/or toxic gases (such as CO₂, O₂, ammonia,
431 sulfur dioxide, chlorine, iodine and cyanogen chloride) due to the physical interaction of
432 functional groups of MOFs. Therefore, specific chemistry of MOFs needs to be specified for
433 any practical application in AQM.

434 The functional tailorability of MOFs is recognized as a great merit to offer improved
435 performance for capturing and storage of gaseous pollutants over conventional materials (such as
436 MEA, activated carbon, or other filtration media). In addition, direct and low cost functional and
437 hierarchical pore structures of MOFs are desirable for developing novel approaches for post
438 synthetic modification (such as controlled etching). Such applications may open a great
439 opportunity for their practical implementation at industrial scale. It is anticipated that in the near
440 future, research and development on MOFs will find its special need to fulfill various demands
441 for AQM.

442

443

444 **Acknowledgements**

445 This study was supported by a grant from the National Research Foundation of Korea (NRF)
446 funded by the Ministry of Education, Science, and Technology (MEST) (No. 2009-0093848).
447 The third author also acknowledges the support made by a National Research Foundation of
448 Korea (NRF) Grant funded by the Korean Government (MSIP) (No. 2914RA1A004893).

449

450

451 **BIOGRAPHIES**

Dr. Pawan Kumar obtained his Ph.D. (Engineering) from the Academy of Scientific and Innovative Research - Central Scientific Instruments Organization (AcSIR-CSIO), Chandigarh (India). He has more than one year of post-Ph.D. experience in the fields of nanotechnology, analytical and environmental engineering and is currently involved in the different projects such as development of novel electrode materials for high energy density storage devices, sensors, porous materials based environmental, and clinical applications. His research interests also include the synthesis and applications of carbon based

462 nanostructures, quantum dots, metal organic frameworks and their nanocomposites. He has
463 published over 15 scholarly articles in SCI journals.

464
465

Prof. Ki-Hyun was at Florida University for an M.S. in 1986 and received a PhD from Marine & Atmospheric Science at University of South Florida in 1992. He was a Research Associate at Oak Ridge National Lab., USA from 1992 to 1994 and then an Assistant Professor at the Sang Ji University, S. Korea from 1995 to 1998. In 1999, he joined the Dept of

473 Environment & Energy, Sejong University, S. Korea from 2008 to 2013. In 2014, he moved to
474 Dept. of Civil and Environmental Engineering at Hanyang University, S. Korea. His research
475 areas focus on the environmental analysis and air quality management of various odorants and
476 toxic pollutants. He was awarded a National Star Faculty offered by the Korean Ministry of
477 Education, Science and Technology in 2006. He is currently serving as editorial members of
478 journals like Sensors, Scientific World, and several others. He has published more than 350
479 articles in peer-reviewed international SCI journals.

480

481

482



483 **Prof. Kwon** completed his Ph.D. in the Department of Earth
484 and Environmental Engineering at Columbia University,
485 New York, USA in 2008. Immediately following, Prof.
486 Kwon was appointed as Associated Research Scientist at the
487 Earth Engineering Center of the Earth Institute at Columbia
488 University. Afterwards, Prof. Kwon returned to South Korea
489 and worked at the Research Institute of Industrial Science
490 and Technology (RIST) from 2010 to 2013. In 2013, Prof.
491 Kwon joined as a faculty member in the Department of
492 Environment and Energy at Sejong University. His research

493 interests are focused on combustion, catalysis, fuel processing, bioenergy, and air pollution
494 controls. To date, he published more than 50 articles in peer-reviewed international SCI journals.

495

496



497 **Prof. Jan E. Szulejko** received the B.Sc. degree from the
498 University of Wales, Cardiff, U.K., in physics (cum laude, 1974)
499 and chemistry (cum laude, 1977). In 1981, he received the Ph.D.
500 degree in negative ion mass spectrometry from the University of
501 Wales. From 1982 to 1998 at the University of Waterloo, Canada,
502 he studied various aspects of ion-molecule reactions and ion
503 thermochemistry. He is the lead co-author of a 1993 seminal

504 paper on the proton affinity scale (J. Am. Chem. Soc., vol. 115, pp. 7839–7848, >335 citations).

505 He has modified and built a number of mass spectrometers. In January 2001, he first joined the

506 research group of Prof. T. Solouki at the University of Maine (Orono), U.S.A. to work on the
507 interfacing of a gas chromatograph (GC) to an FT-ICR MS (GC/FT-ICR MS) for environmental
508 and breath analysis. He is the lead co-author of a 2010 review on the efficacy of breath analysis
509 for cancer diagnosis (IEEE Sensors J., vol. 10, pp 185-210). In 2012, he joined as a research
510 professor the research group of Prof. K.-H. Kim at Sejong University, Seoul, S. Korea. In 2014,
511 he moved to Hanyang University with Prof. K.-H. Kim's laboratory and is currently a professor.
512 Since 2012, his research interests include air quality management, air pollution, climate change,
513 quantification of compounds lacking authentic standards and surrogates (CLASS), and sorbent
514 performance. He has published over 60 scholarly articles in SCI journals.

515 References

- 516 [1] Front-matter. In: Pohanish RP, editor. Sittig's Handbook of Toxic and Hazardous Chemicals and
517 Carcinogens (Sixth Edition). *Oxford: William Andrew Publishing*; 2012, i-iii.
- 518 [2] J. A. Bernstein, N. Alexis, C. Barnes, I. L. Bernstein, A. Nel, D. Peden, D. Diaz-Sanchez, S. M.
519 Tarlo, P. B. Williams, *Journal of Allergy and Clinical Immunology* 2004, **114**, 1116.
- 520 [3] R. Mitchell, F. Popham, *The Lancet* 2008, **372**, 1655.
- 521 [4] NIOSH Pocket Guide to Chemical Hazards. Cincinnati, OH: U.S. Department of Health and
522 Human Services, Public Health Service, and Centers for Disease Control, National Institute for
523 Occupational Safety and Health, DHHS (NIOSH). 2005, publication no. 2005-149.
- 524 [5] Health Effects Notebook for Hazardous Air Pollutants by US-EPA, Available online from
525 19.10.2013 at: <http://www.epa.gov/ttn/atw/hlthef/hapindex.html>. Last Access 19.08.2015.
- 526 [6] K.H. Kim, S. A. Jahan, E. Kabir, *TrAC Trends in Analytical Chemistry* 2012, **33**, 1.
- 527 [7] K.H. Kim, S. A. Jahan, E. Kabir, *Environment International* 2013, **59**, 41.
- 528 [8] E. Barea, C. Montoro, J. A. R. Navarro, *Chemical Society Reviews* 2014, **43**, 5419.
- 529 [9] J. B. DeCoste, G. W. Peterson, *Chemical Reviews* 2014, **114**, 5695.
- 530 [10] M. J. Rosseinsky, M. W. Smith, C. M. Timperley, *Nature Materials* 2015, **14**, 469.
- 531 [11] S. Aguado, A. C. Polo, M. A. P. Bernal, J. n. Coronas, J. Santamaría, *Journal of Membrane*
532 *Science* 2004, **240**, 159.
- 533 [12] M. Ranocchiari, J. A. Van Bokhoven, *Physical Chemistry Chemical Physics* 2011, **13**, 6388-
534 6396.
- 535 [13] Y. Belmabkhout, R. S. Guerrero, A. Sayari, *Chemical Engineering Science* 2010, **65**, 3695.
- 536 [14] S. U. Rege, R. T. Yang, M. A. Buzanowski, *Chemical Engineering Science* 2000, **55**, 4827.
- 537 [15] J. K. Stolaroff, D. W. Keith, G. V. Lowry, *Environmental Science & Technology* 2008, **42**,
538 2728.
- 539 [16] V. Nikulshina, C. Gebald, A. Steinfeld, *Chemical Engineering Journal* 2009, **146**, 244.
- 540 [17] A. Goepfert, M. Czaun, G. K. S. Prakash, G. A. Olah, *Energy & Environmental Science* 2012,
541 **5**, 7833.
- 542 [18] G. Férey, C. Mellot-Draznieks, C. Serre, F. Millange, *Accounts of Chemical Research* 2005,
543 **38**, 217.
- 544 [19] C. Serre, C. Mellot-Draznieks, S. Surblé, N. Audebrand, Y. Filinchuk, G. Férey, *Science* 2007,
545 **315**, 1828.
- 546 [20] L. E. Kreno, K. Leong, O. K. Farha, M. Allendorf, R. P. Van Duyne, J. T. Hupp, *Chemical*
547 *Reviews* 2011, **112**, 2, 1105.
- 548 [21] P. Kumar, A. Deep, K. H. Kim, R. J. Brown, *TrAC Trends in Analytical Chemistry* 2015, **11**,
549 39.

- 550 [22] P. Falcaro, R. Ricco, C. M. Doherty, K. Liang, A. J. Hill, M. J. Styles, *Chemical Society*
551 *Reviews* 2014, **43**, 5513.
- 552 [23] P. Kumar, A. Deep, K. H. Kim, R. J. Brown, *Progress in Polymer Science* 2015, **45**,105.
- 553 [24] C. Yang, U. Kaipa, Q. Z. Mather, X. Wang, V. Nesterov, A. F. Venero, M. A. Omary, *Journal*
554 *of the American Chemical Society* 2011, **133**, 18094.
- 555 [25] A. Corma, H. Garcia, F. Llabrés, I. Xamena, *Chemical Reviews* 2010, **110**, 4606.
- 556 [26] G. Férey, C. Serre, T. Devic, G. Maurin, H. Jobic, P. L. Llewellyn, G. De Weireld, A. Vimont,
557 M. Daturi, J.-S. Chang, *Chemical Society Reviews* 2011, **40**, 550.
- 558 [27] P. Nugent, Y. Belmabkhout, S. D. Burd, A. J. Cairns, R. Luebke, K. Forrest, T. Pham, S. Ma,
559 B. Space, L. Wojtas, M. Eddaoudi, M. J. Zaworotko, *Nature* 2013, **495**, 80.
- 560 [28] O. Shekhah, Y. Belmabkhout, Z. Chen, V. Guillerm, A. Cairns, K. Adil, M. Eddaoudi, *Nature*
561 *Communications* 2014, **5**, 4228.
- 562 [29] N. Stock, S. Biswas, *Chemical Reviews* 2011, **112**, 933.
- 563 [30] S. M. Cohen, *Chemical Reviews*. 2012, **112**,970.
- 564 [31] T. G. Glover, G. W. Peterson, B. J. Schindler, D. Britt, O. Yaghi, *Chemical Engineering*
565 *Science* 2011, **66**, 163.
- 566 [32] N. A. Khan, Z. Hasan, S. H. Jhung, *Journal of Hazardous Materials* 2013, **244**, 444.
- 567 [33] H. Furukawa, K. E. Cordova, M. O’Keeffe, O. M. Yaghi, *Science* 2013, **341**, 1230444.
- 568 [34] H. Deng, C. J. Doonan, H. Furukawa, R. B. Ferreira, J. Towne, C. B. Knobler, B. Wang, O. M.
569 Yaghi, *Science* 2010, **327**, 846.
- 570 [35] P. S. Crespo, E. Gobechiya, E. V. Ramos Fernandez, J. J. Alcanniz, A. Martinez-Joaristi, E.
571 Stavitski, C. E. Kirschhock, J. A. Martens, F. Kapteijn, J. Gascon, *Langmuir* 2012, **28**, 12916.
- 572 [36] T. Lescouet, E. Kockrick, G. Bergeret, M. Pera-Titus, S. Aguado, D. Farrusseng, *Journal of*
573 *Materials Chemistry* 2012, **22**, 10287.
- 574 [37] O. Shekhah, J. Liu, R. Fischer, C. Woll, *Chemical Society Reviews* 2011, **40**, 1081.
- 575 [38] C. M. Doherty, G. Greci, R. Ricco, J. I. Mardel, J. Reboul, S. Furukawa, S. Kitagawa, A. J.
576 Hill, P. Falcaro, *Advanced Materials* 2013, **25**, 4701.
- 577 [39] M. Alhamami, H. Doan, C.H. Cheng, *Materials* 2014, **7**, 3198-3250.
- 578 [40] T. Rodenas, I. Luz, G. Prieto, B. Seoane, H. Miro, A. Corma, F. Kapteijn, F. X. L. I. Xamena,
579 J. Gascon, *Nature Materials* 2015, **14**, 48.
- 580 [41] Web link: <http://jclfss.weebly.com/design-and-cost.html> (Accessed: Oct 2015).
- 581 [42] BASF, "BASF BasoliteHandout", 2005.
- 582 [43] R. J. Kuppler, D. J. Timmons, Q. R. Fang, J. R. Li, T. A. Makal, M. D. Young, H. C.
583 Zhou, *Coordination Chemistry Reviews* 2009, **253(23)**, 3042.
- 584 [44] X. Wang, J. Zhou, H. Fu, W. Li, X. Fan, G. Xin, J. Zheng, X. Li, *Journal of Materials*
585 *Chemistry A* 2014, **2**, 14064.
- 586 [45] J. Liu, L. Chen, H. Cui, J. Zhang, L. Zhang, C.Y. Su, *Chemical Society Reviews* 2014, **43**,
587 6011.
- 588 [46] C. J. Brown, F. D. Toste, R. G. Bergman, K. N. Raymond, *Chemical Reviews* 2015, **115**, 3012.
- 589 [47] S. Choi, J. H. Drese, C. W. Jones, *ChemSusChem* 2009, **2**, 796.
- 590 [48] J.-R. Li, J. Sculley, H. C. Zhou, *Chemical Reviews* 2011, **112**, 869.
- 591 [49] K. Sumida, D. L. Rogow, J.A. Mason, T.M. McDonald, E.D. Bloch, Z.R. Herm, *Chemical*
592 *Reviews*. 2011,**112**,724.
- 593 [50] M.P. Suh, H. J. Park, T.K. Prasad, D.W Lim, *Chemical Reviews*. 2011,**112**,782.
- 594 [51] R. B. Getman, Y. S. Bae, C. E. Wilmer, R. Q. Snurr, *Chemical Reviews* 2011, **112**, 703.
- 595 [52] S. Deng, *Encyclopedia of Chemical Processing* (Print Version): CRC Press; 2005. p. XLV-
596 XLVI.
- 597 [53] C. Lu, H. Bai, B. Wu, F. Su, J. F. Hwang, *Energy & Fuels* 2008, **22**, 3050.
- 598 [54] S. Wu, T. Beum, J. Yang, J. Kim, *Industrial & Engineering Chemistry Research* 2007, **46**,
599 7896.

- 600 [55] E. P. Reddy, P. G. Smirniotis, *The Journal of Physical Chemistry B* 2004, **108**, 7794.
601 [56] R. V. Siriwardane, M.-S. Shen, E. P. Fisher, J. Losch, *Energy & Fuels* 2005, **19**, 1153.
602 [57] N. Hiyoshi, K. Yogo, T. Yashima, *Microporous and Mesoporous Materials* 2005, **84**, 357.
603 [58] M. Kato, S. Yoshikawa, K. Nakagawa, *Journal of Materials Science Letters* 2002, **21**, 485.
604 [59] M. Plaza, C. Pevida, A. Arenillas, F. Rubiera, J. Pis, *Fuel* 2007, **86**, 2204.
605 [60] N. C. Burtch, H. Jasuja, K. S. Walton, *Chemical Reviews* 2014, **114**, 10575.
606 [61] C. Xiao, Z. Chu, X.-M. Ren, T.-Y. Chen, W. Jin, *Chemical Communications* 2015, **51**, 7947.
607 [62] J. S. Oh, W. G. Shim, J. W. Lee, J. H. Kim, H. Moon, G. Seo, *Journal of Chemical &*
608 *Engineering Data* 2003, **48**, 1458.
609 [63] Z. Hasan, S. H. Jhung, *Journal of Hazardous Materials* 2015, **283**, 329.
610 [64] K.S. Sing, *Pure and Applied Chemistry*. 1985, **57**,603.
611 [65] For more information see <http://www.iupac.org/web/ins/2010-009-1-100>.
612 [66] J. Canivet, A. Fateeva, Y. Guo, B. Coasne, D. Farrusseng, *Chemical Society Reviews* 2014, **43**,
613 5594.
614 [67] F. O. X. Coudert, A. Boutin, A. H. Fuchs, A. V. Neimark, *The Journal of Physical Chemistry*
615 *Letters* 2013, **4**, 3198.
616 [68] S. Keskin, T. M. Van Heest, D. S. Sholl, *ChemSusChem* 2010, **3**, 879.
617 [69] B. Seoane, J. Coronas, I. Gascon, M. E. Benavides, O. Karvan, J. Caro, F. Kapteijn, J. Gascon,
618 *Chemical Society Reviews* 2015, **44**, 2421.
619 [70] D. M. D'Alessandro, B. Smit, J. R. Long, *Angewandte Chemie International Edition* 2010, **49**,
620 6058.
621 [71] A. Demessence, D. M. D'Alessandro, M. L. Foo, J. R. Long, *Journal of the American*
622 *Chemical Society* 2009, **131**, 8784.
623 [72] D. Britt, H. Furukawa, B. Wang, T. G. Glover and O. M. Yaghi, *Proceedings of the National*
624 *Academy of Sciences* 2009, **106**, 20637.
625 [73] H. He, Y. Song, C. Zhang, F. Sun, R. Yuan, Z. Bian, L. Gao, G. Zhu, *Chemical*
626 *Communications* 2015, **51**, 9463.
627 [74] D. Saha, Z. Bao, F. Jia, S. Deng, *Environmental Science & Technology* 2010, **44**, 1820.
628 [75] S. Gadipelli, Z. Guo, *Chemistry of Materials* 2014, **26**, 6333.
629 [76] A.O. Yazaydin, I.A. Benin, A.S. Faheem, P. Jakubczak, J.J. Low, R.R. Willis, Q.R. Snurr,
630 *Chemistry of Materials* 2009, **21**(8),1425.
631 [77] A. F. Ferreira, A. M. Ribeiro, S. Kulaç, A. E. Rodrigues, *Chemical Engineering Science* 2014,
632 **124**, 79.
633 [78] W. R. Lee, S. Y. Hwang, D. W. Ryu, K. S. Lim, S. S. Han, D. Moon, J. Choi, C. S. Hong,
634 *Energy & Environmental Science* 2014, **7**, 744.
635 [79] S. Choi, T. Watanabe, T.H. Bae, D. S. Sholl, C. W. Jones, *The Journal of Physical Chemistry*
636 *Letters* 2012, **3**, 1136.
637 [80] T. M. McDonald, J. A. Mason, X. Kong, E. D. Bloch, D. Gygi, A. Dani, V. Crocellà, F.
638 Giordanino, S. O. Odoh, W. S. Drisdell, *Nature* 2015, **519**, 303.
639 [81] C. Wang, L. Li, S. Tang, X. Zhao, *ACS Applied Materials & Interfaces* 2014, **6** 16932.
640 [82] D.M. Chen, N. Xu, X.H. Qiu, P. Cheng, *Crystal Growth & Design* 2015, **15**,961.
641 [83] S. R. Caskey, A. G. Wong-Foy, A. J. Matzger, *Journal of the American Chemical Society*
642 2008, **130**, 10870.
643 [84] M. Eddaoudi, J. Kim, N. Rosi, D. Vodak, J. Wachter, M. O'Keeffe, O. M. Yaghi, *Science* 2002,
644 **295**, 469.
645 [85] T. Duren, L. Sarkisov, O. M. Yaghi, R. Q. Snurr, *Langmuir* 2004, **20**, 2683.
646 [86] H. Frost, T. Düren, R. Q. Snurr, *The Journal of Physical Chemistry B* 2006, **110**, 9565.
647 [87] S. Keskin, *Molecular Dynamics - Theoretical Developments and Applications in*
648 *Nanotechnology and Energy* 2012. Prof. Lichang Wang (Ed.), ISBN: 978-953-51-0443-8, InTech,
649 DOI: 10.5772/35925.
650 [88] K. C. Kim, D. Yu, R. Q. Snurr, *Langmuir* 2013, **29**, 1446-1456.
651 [89] K. C. Kim, P. Z. Moghadam, D. Fairen-Jimenez, R. Q. Snurr, *Industrial & Engineering*
652 *Chemistry Research* 2015 **54**, 3257.

- 653 [90] C. Petit, L. Huang, J. Jagiello, J. Kenvin, K. E. Gubbins, T. J. Bandosz, *Langmuir* 2011, **27**
654 13043.
- 655 [91] D. Britt, D. Tranchemontagne, O. M. Yaghi, *Proceedings of the National Academy of Sciences*
656 2008, **105**, 11623.
- 657 [92] D. Saha, S. Deng, *Journal of Colloid and Interface Science* 2010, **348**, 615.
- 658 [93] I. Spanopoulos, P. Xydias, C. D. Malliakas, P. N. Trikalitis, *Inorganic Chemistry* 2013, **52**,
659 855-862.
- 660 [94] H. Jasuja, G. W. Peterson, J. B. Decoste, M. A. Browe, K. S. Walton, *Chemical Engineering*
661 *Science* 2014, **124**, 118.
- 662 [95] J.L. Murray, M. Dinca, J Yano, S. Chavan, S. Bordiga, M. Brown, R.J. Long, *Journal of the*
663 *American Chemical Society* 2010, **132(23)**, 7856.
- 664 [96] D.E. Bloch, J.L. Murray, L.W. Queen, S. Chavan, N.S. Maximoff, P.J. Bigi, *Journal of the*
665 *American Chemical Society* 2011, **133(37)** 14814.
- 666 [97] D. F. Sava Gallis, M. V. Parkes, J. A. Greathouse, X. Zhang, T. M. Nenoff, *Chemistry of*
667 *Materials* 2015, **27**, 2018.
- 668 [98] E. Haque, J. E. Lee, I. T. Jang, Y. K. Hwang, J.S. Chang, J. Jegal, S. H. Jhung, *Journal of*
669 *Hazardous Materials* 2010, **181**, 535.
- 670 [99] H.R. Fu, F. Wang, J. Zhang, *Dalton Transactions* 2015, **44**, 2893.
- 671 [100] E. Haque, J. W. Jun, S. H. Jhung, *Journal of Hazardous Materials* 2011, **185**, 507
- 672 [101] Z. Hasan, M. Tong, B. K. Jung, I. Ahmed, C. Zhong, S. H. Jhung, *The Journal of Physical*
673 *Chemistry C* 2014, **118**, 21049 .
- 674 [102] F. Leng, W. Wang, X. J. Zhao, X. L. Hu, Y. F. Li, *Colloids and Surfaces A: Physicochemical*
675 *and Engineering Aspects* 2014, **441**, 164.
- 676 [103] C. Chen, M. Zhang, Q. Guan, W. Li, *Chemical Engineering Journal* 2012, **183**, 60.
- 677 [104] E. Haque, V. Lo, A. I. Minett, A. T. Harris, T. L. Church, *Journal of Materials Chemistry A*
678 2014, **2**, 193.
- 679 [105] G. W. Peterson, J. A. Rossin, J. B. DeCoste, K. L. Killops, M. Browe, E. Valdes, P. Jones,
680 *Industrial & Engineering Chemistry Research* 2013, **52**, 5462.
- 681 [106] C. Wang, Z. Xie, K. E. deKrafft, W. Lin, *Journal of the American Chemical Society* 2011,
682 **133**, 13445
- 683 [107] L. Shen, S. Liang, W. Wu, R. Liang, L. Wu, *Dalton Transactions* 2013, **42**, 13649-13657.
- 684 [108] J. J. Du, Y.P. Yuan, J.X. Sun, F.M. Peng, X. Jiang, L.G. Qiu, A.J. Xie, Y.H. Shen, J.F. Zhu,
685 *Journal of Hazardous Materials* 2011, **190**, 945.
- 686 [109] F. Hincal, P.F Erkekoglu, *Jornal of Pharmaceutical Science* 2006, **31**,220.
- 687 [110] J. E. Mondloch, M. J. Katz, W. C. Isley III, P. Ghosh, P. Liao, W. Bury, G. W. Wagner, M.
688 G. Hall, J. B. DeCoste, G. W. Peterson, *Nature Materials* 2015, **14**, 512.
- 689 [111] G. W. Peterson, J. A. Rossin, J. B. DeCoste, K. L. Killops, M. Browe, E. Valdes, P. Jones,
690 *Industrial & Engineering Chemistry Research* 2013, **52**, 5462-5469.
- 691 [112] L. Bromberg, Y. Klichko, E. P. Chang, S. Speakman, C. M. Straut, E. Wilusz, T. A. Hatton,
692 *ACS Applied Materials & Interfaces* 2012, **4**, 4595.
- 693 [113] F.J. Ma, S.X. Liu, C.Y. Sun, D.D. Liang, G.J. Ren, F. Wei, Y.G. Chen, Z.M.Su, *Journal of the*
694 *American Chemical Society* 2011, **133**, 4178.
- 695 [114] Y. Liu, P. Gao, C. Huang, Y. Li, *Science China Chemistry* 2015, **1**.
- 696 [115] H. Gao, Y. Luan, K. Chaikittikul, W. Dong, J. Li, X. Zhang, D. Jia, M. Yang, G. Wang, *ACS*
697 *Applied Materials & Interfaces* 2015, **7**, 4667.
- 698 [116] G. Férey, C. Mellot-Draznieks, C. Serre, F. Millange, J. Dutour, S. Surblé, I. Margiolaki,
699 *Science* 2005, **309**, 2040.
- 700 [117] Y. Izumi, *Coordination Chemistry Reviews* 2013, **257**,1, 171.
- 701 [118] NIST Chemistry WebBook (<http://webbook.nist.gov/chemistry/>, accessed June 2015).
- 702 [119] O. K. Varghese, M. Paulose, T. J. LaTempa, C. A. Grimes, *Nano Letters* 2009, **9(2)**, 731.
- 703 [120] J. Cejka, A. Corma, S. Zones, *Zeolites and catalysis: synthesis, reactions and applications*,
704 John Wiley & Sons, 2010.
- 705 [121] M. H. Beyzavi, C. J. Stephenson, Y. Liu, O. Karagiari, J. T. Hupp, O. K. Farha, *Frontiers in*
706 *Energy Research* 2015, **2**.

707

Figure captions

708 **Figure 1.** Different categories of materials, their applications and challenges.¹² Reproduced
709 from Ref. 12 with permission, Copyright © 2011, Royal Society of Chemistry.

710 **Figure 2 (a-f).** Different mechanisms of MOFs for adsorptive removal of hazardous materials
711 in MOFs.⁶³ Reproduced from Ref. 63 with permission, Copyright © 2015, Elsevier Ltd.

712 **Figure 3.** IUPAC report (1985) (A) classification of adsorption isotherm and (B) hysteresis
713 loops.^{60,64} Reproduced from Ref. 49 with permission, Copyright © 2014, American Chemical
714 Society.

715 **Figure 4.** Diamine appended metal organic framework based cooperative insertion
716 mechanism for CO₂ adsorption.⁷⁸ Reproduced from Ref. 78 with permission, Copyright ©
717 2014, Nature Publishing Group.

718 **Figure 5. (A & B)** Chemical structure of IRMOF-6 in which Zn (blue polyhedra), O (red
719 spheres), C (black spheres), Br (green spheres in 2), amino-groups (blue spheres in 3), and
720 **(B)** IRMOF-6 voluminous uptake of methane sorption isotherm fitted at 298 K with
721 Langmuir equation in the pressure range 0 to 42.⁸⁴ Reproduced from Ref. 84 with permission,
722 Copyright © 2002, The American Association for the Advancement of Science.

723 **Figure 6 (A & B)** Schematic representation of straight Forward Route for the Development
724 of Functionalized MOF, and (B) –NH₃ adsorption (filled symbols) and desorption (blank
725 symbols) isotherm by DUT-6 at 1bar.⁹¹ Reproduced from Ref. 91 with permission, Copyright
726 © 2013, American Chemical Society.

727 **Figure 7 (a-e)** (a) SEM-EDS mapping of the metal-exchanged series and their corresponding
728 elemental distribution of (a) Mn (red), (b) Fe (red), (c) Co (red) ; and (d and e) N₂ and O₂
729 adsorption isotherms measured at 273, 283, and 298 K.⁹⁷ Reproduced from Ref. 97 with
730 permission, Copyright © 2015, American Chemical Society.

731 **Figure 8 (A, B & C)** The cage sub-structure of FIR-51, (B) (a) Small hydrocarbons and CO₂
732 sorption isotherms of FIR-51 at 273 K; and (C) small hydrocarbons and CO₂ sorption
733 isotherms at 294 K.⁹⁹ Reproduced from Ref. 99 with permission, Copyright © 2011, Royal
734 Society of Chemistry.

735 **Figure 9 (A-D)** Graphical representation of pyridine by NH₂- functionalized UIO-66 (B,C,
736 and D), showing the effect on adsorption process of different temperature (45, 50 and 60
737 °C).¹⁰¹ Reproduced from Ref. 101 with permission, Copyright © 2014, American Chemical
738 Society.

739 **Figure 10 (A & B)** Cu-BTC color changes during exposure ammonia, arsine, and hydrogen
740 sulfide, and (B) Cu-BTC based packed bed breakthrough testing for (a) ammonia, (b) arsine,
741 and (c) hydrogen sulfide, and (d) concentration time (Ct) values to break.¹⁰⁵ Reproduced from
742 Ref. 105 with permission, Copyright © 2015, American Chemical Society.

743 **Figure 11. (A, B & C)** Presence of the potential catalytic sites (A), the postsynthetic
744 modification methods (B), and metal nanoparticles other guest molecules (C) embedded in
745 the cavities (right) of MOFs.⁴⁵ Reproduced from Ref. 45 with permission, Copyright © 2014,
746 Royal Society of Chemistry.

747 **Figure 12.** Catalytic degradation mechanism (hydrolysis and oxidative) pathways for
748 selected CWAs.⁸ Reproduced from Ref. 8 with permission, Creative Commons Attribution
749 3.0 Unported License Copyright © 2014 Royal Society of Chemistry.

750 **Figure 13 (A & B)** Schematic representation of organic photocatalysis through doped MOFs
751 for water oxidation, carbon dioxide reduction, (B) doped [Zr₆O₄(OH)₄(bpdc)₆] (UiO-67)
752 systems and the resulting aerobic catalytic oxidation of thioanisole.¹⁰⁶ Reproduced from Ref.
753 106 with permission, Copyright © 2011, American Chemical Society.

754 **Figure 14. (A & B)** (A) Hydrolysis mechanism of CWAs through utilization of MOFs (B)
755 UV-Vis spectra showing the formation of p-nitrophenoxide via visible-region adsorption

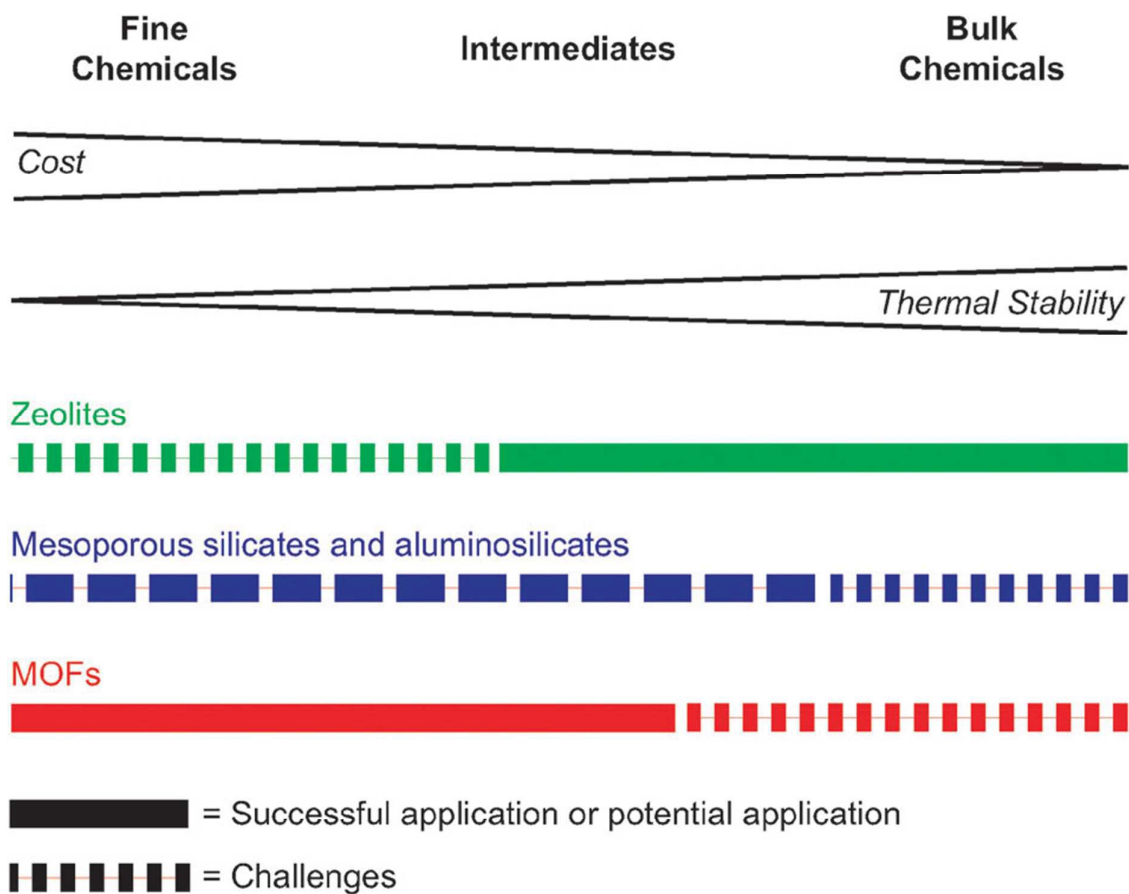
756 spectroscopy at $E_{max} = 407$.¹¹⁰ Reproduced from Ref. 110 with permission, Copyright ©
757 2015, Nature Publishing Group.

758 **Figure 15.** Schematic representation of Sodalite-type porous metal–organic framework with
759 polyoxometalate templates: adsorption and decomposition of dimethyl methylphosphonate.¹¹³
760 Reproduced from Ref. 113 with permission, Copyright © 2011, American Chemical Society.

761

Figures

762 **Figure 1.** Different categories of materials, their applications and challenges.¹² Reproduced
763 from Ref. 12 with permission, Copyright © 2011, Royal Society of Chemistry.



764

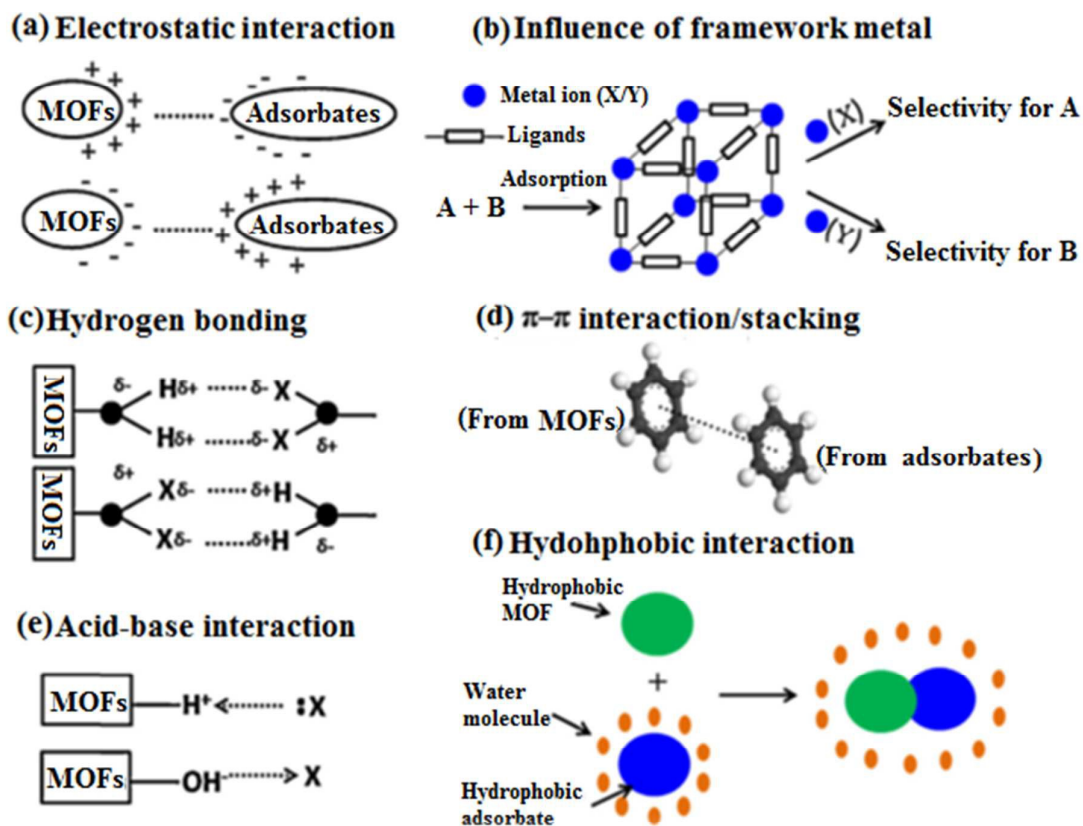
765

766

767

768

769 **Figure 2 (a-f).** Different mechanisms of MOFs for adsorptive removal of hazardous materials
 770 in MOFs.⁶³ Reproduced from Ref. 63 with permission, Copyright © 2015, Elsevier Ltd .
 771

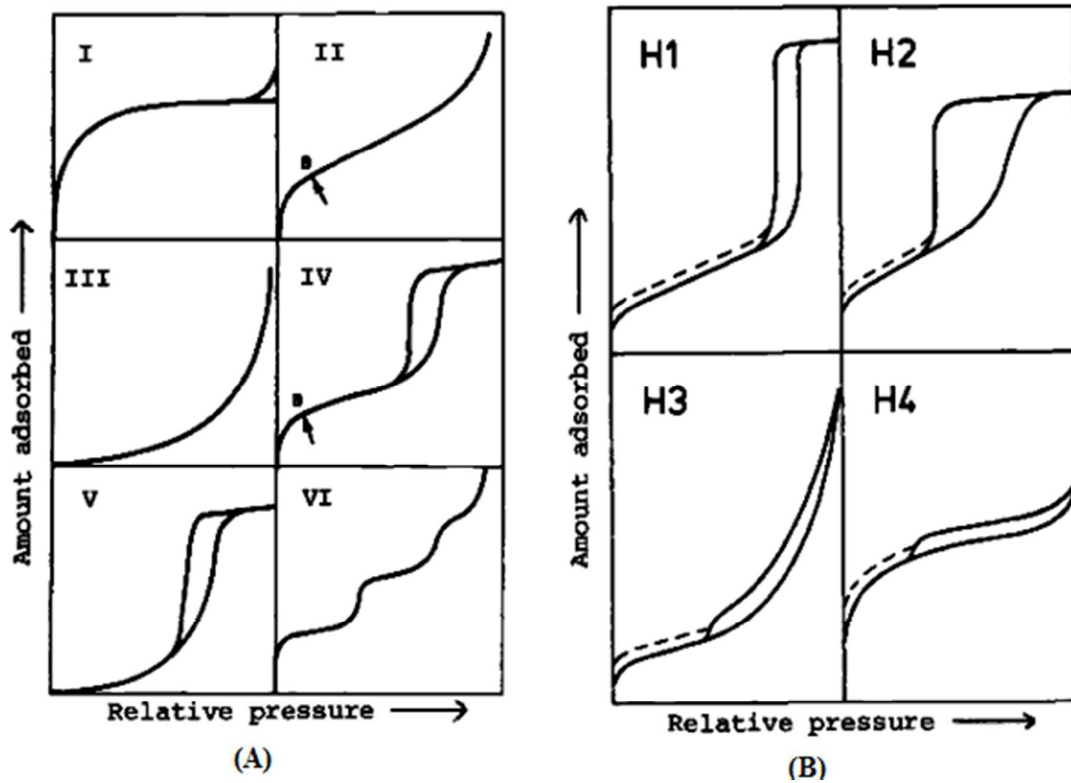


772

773

774 **Figure 3.** IUPAC report (1985) (A) classification of adsorption isotherm and (B) hysteresis
775 loops.^{60,64} Reproduced from Ref. 49 with permission, Copyright © 2014, American Chemical
776 Society.

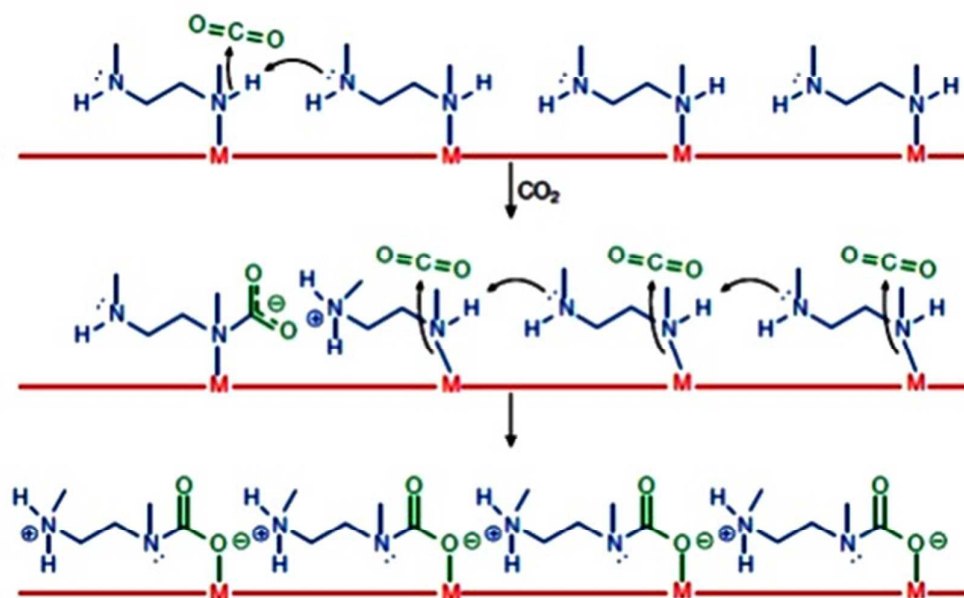
777
778



779

780

781 **Figure 4.** Diamine appended metal organic framework based cooperative insertion
782 mechanism for CO₂ adsorption.⁷⁸ Reproduced from Ref. 78 with permission, Copyright ©
783 2014, Nature Publishing Group.



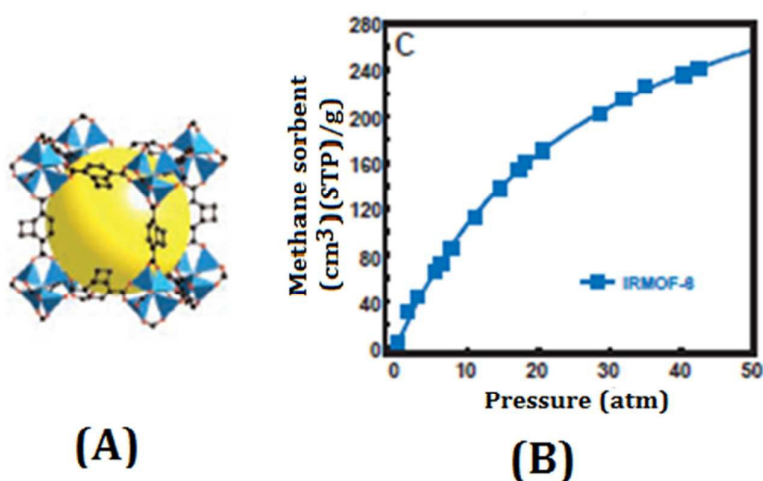
784

785

786 **Figure 5. (A & B)** Chemical structure of IRMOF-6 in which Zn (blue polyhedra), O (red
787 spheres), C (black spheres), Br (green spheres in 2), amino-groups (blue spheres in 3), and
788 **(B)** IRMOF-6 voluminous uptake of methane sorption isotherm fitted at 298 K with
789 Langmuir equation in the pressure range 0 to 42.⁸⁴ Reproduced from Ref. 84 with permission,
790 Copyright © 2002, The American Association for the Advancement of Science.

791

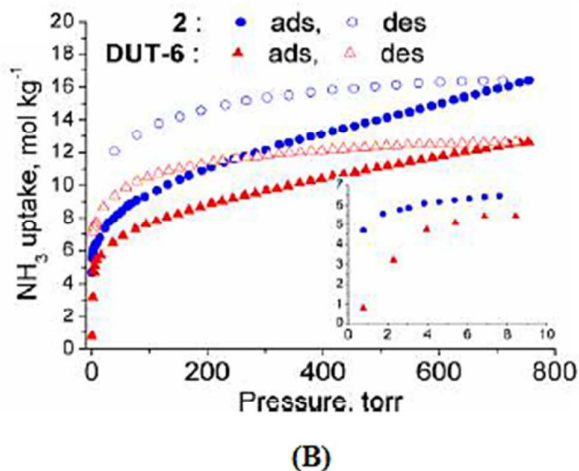
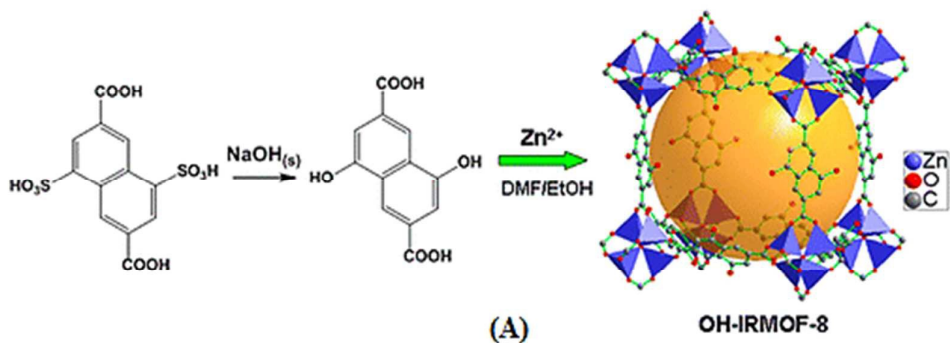
792



793

794

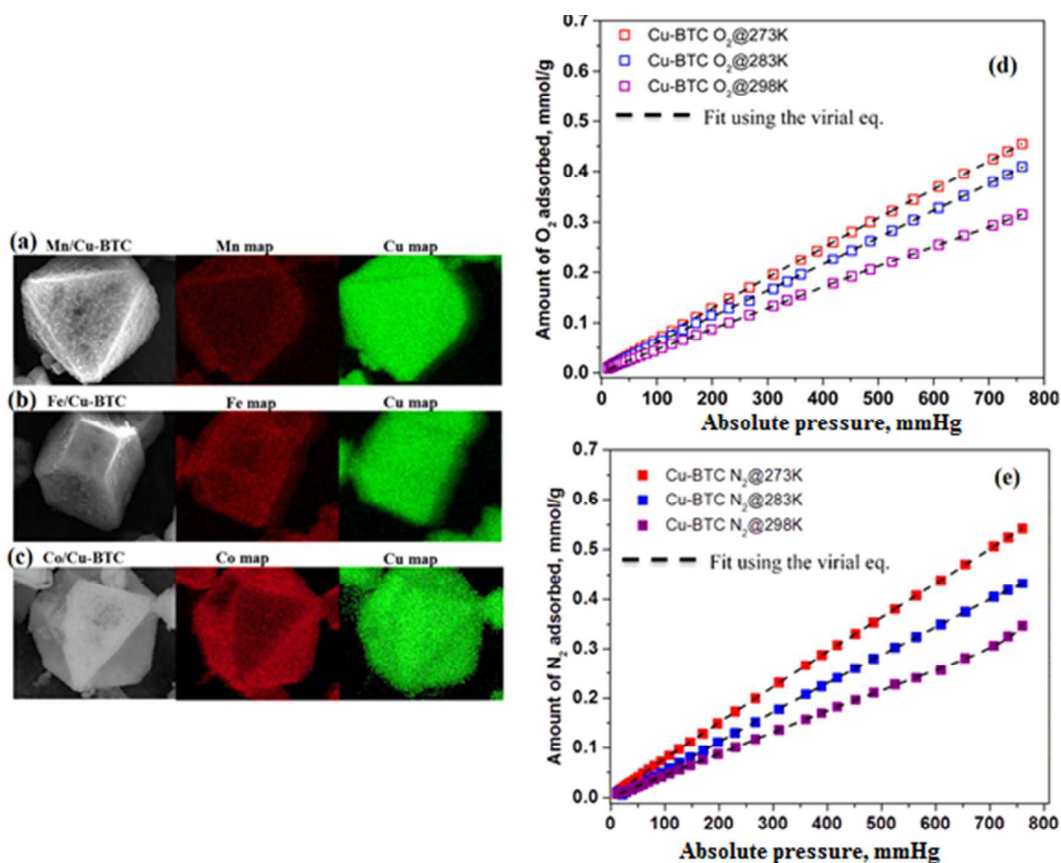
795 **Figure 6 (A & B)** Schematic representation of straight Forward Route for the Development
 796 of Functionalized MOF, and (B) -NH_3 adsorption (filled symbols) and desorption (blank
 797 symbols) isotherm by DUT-6 at 1bar.⁹¹ Reproduced from Ref. 91 with permission, Copyright
 798 © 2013, American Chemical Society.
 799



800

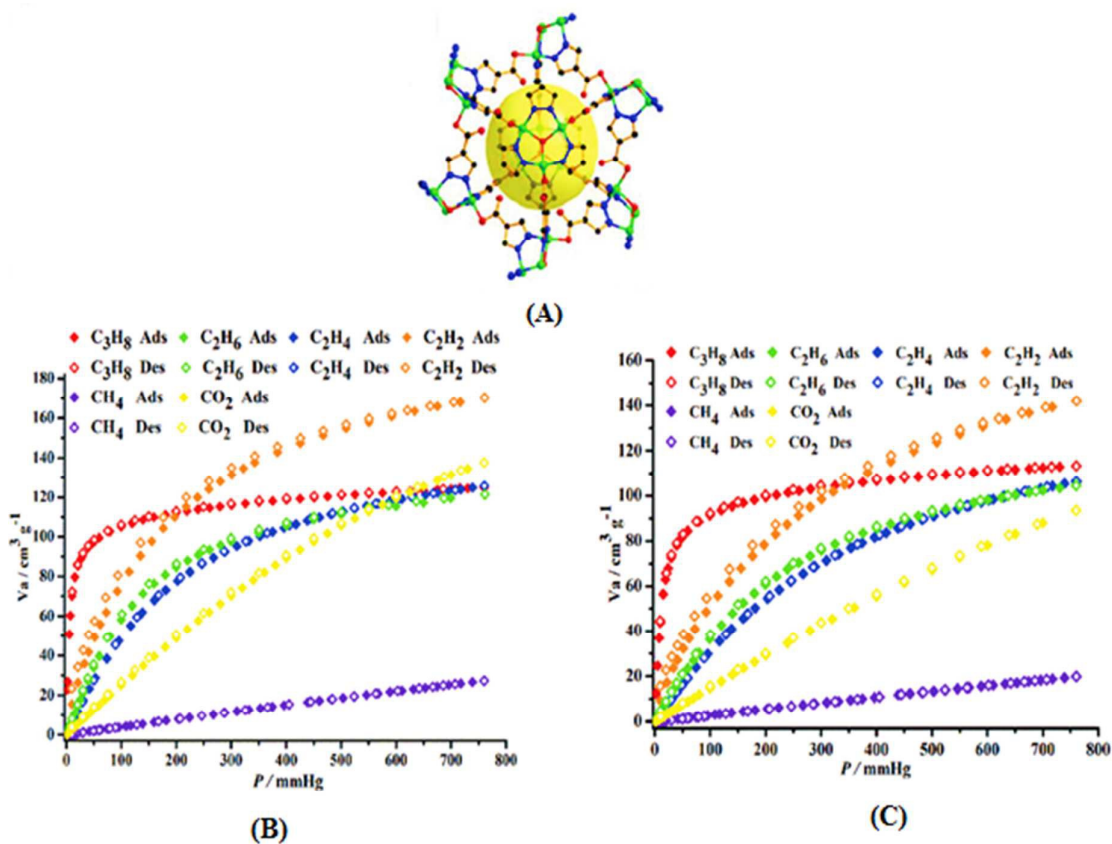
801

802 **Figure 7. (a-e)** (a) SEM-EDS mapping of the metal-exchanged series and their corresponding
803 elemental distribution of (a) Mn (red), (b) Fe (red), (c) Co (red) ; and (d and e) N₂ and O₂
804 adsorption isotherms measured at 273, 283, and 298 K.⁹⁷ Reproduced from Ref. 97 with
805 permission, Copyright © 2015, American Chemical Society.
806



807
808

809 **Figure 8 (A, B & C)** The cage sub-structure of FIR-51, (B) (a) Small hydrocarbons and CO₂
810 sorption isotherms of FIR-51 at 273 K; and (C) small hydrocarbons and CO₂ sorption
811 isotherms at 294 K.⁹⁹ Reproduced from Ref. 99 with permission, Copyright © 2011, Royal
812 Society of Chemistry.

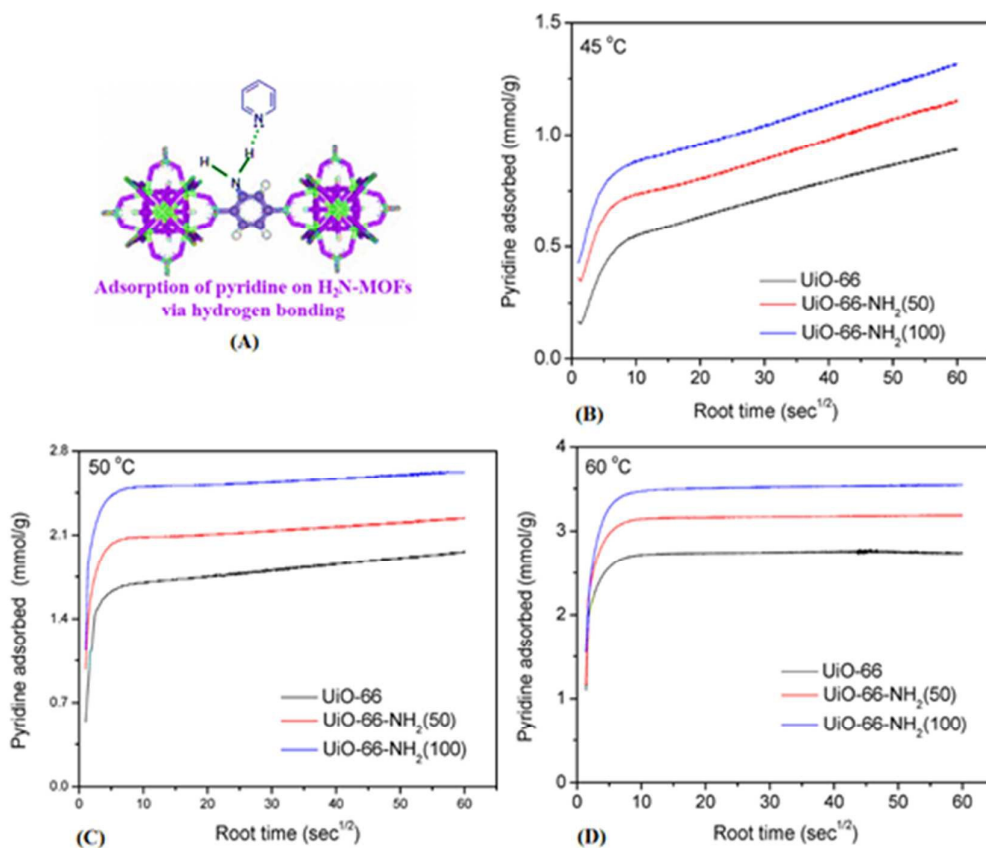


813

814

815

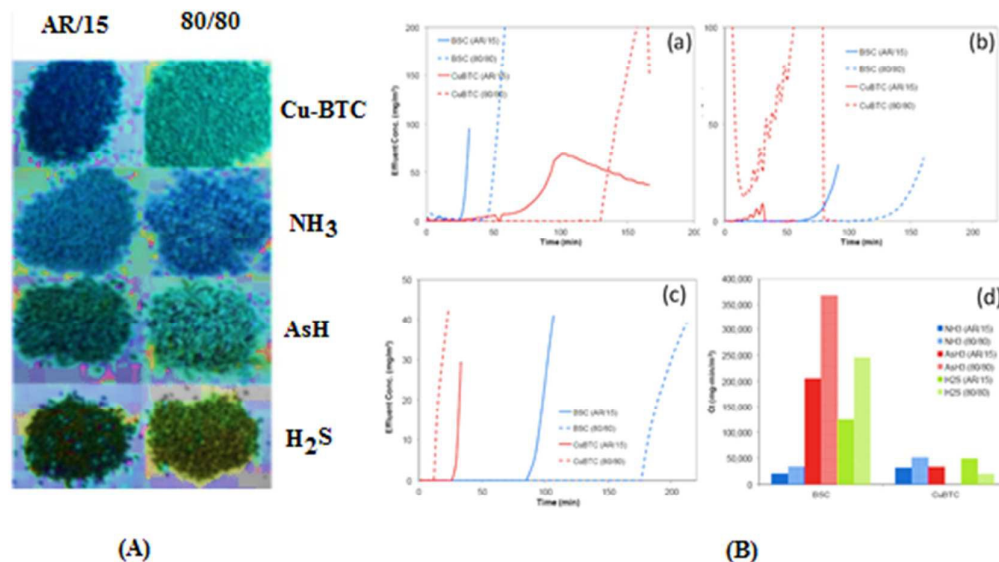
816 **Figure 9 (A-D)** Graphical representation of pyridine by NH_2 - functionalized UiO-66 (B,C,
817 and D), showing the effect on adsorption process of different temperature (45, 50 and 60
818 $^\circ\text{C}$).¹⁰¹ Reproduced from Ref. 101 with permission, Copyright © 2014, American Chemical
819 Society.



820

821

822 **Figure 10 (A & B)** Cu-BTC color changes during exposure ammonia, arsine, and hydrogen
 823 sulfide, and (B) Cu-BTC based packed bed breakthrough testing for (a) ammonia, (b) arsine,
 824 and (c) hydrogen sulfide, and (d) concentration time (Ct) values to break.¹⁰⁵ Reproduced from
 825 Ref. 105 with permission, Copyright © 2015, American Chemical Society.
 826



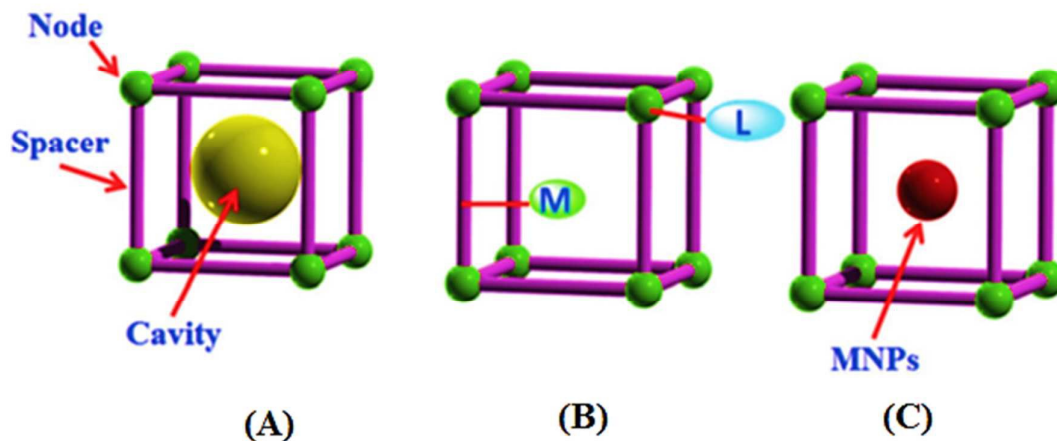
827

828

829 **Figure 11.** (A, B & C) Presence of the potential catalytic sites (A), the postsynthetic
830 modification methods (B), and metal nanoparticles other guest molecules (C) embedded in
831 the cavities (right) of MOFs.⁴⁵ Reproduced from Ref. 45 with permission, Copyright © 2014,
832 Royal Society of Chemistry.

833

834

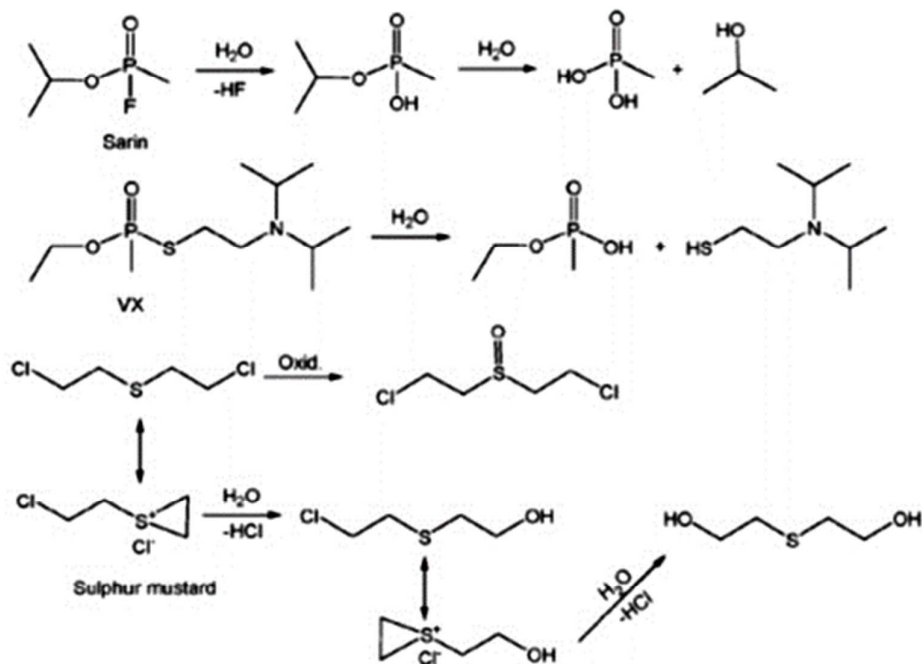


835

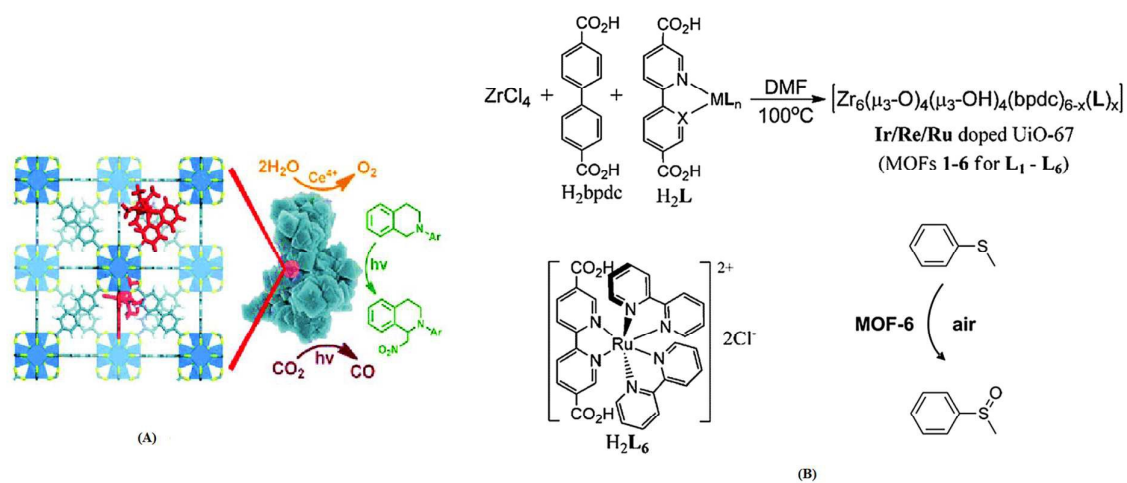
836

837 **Figure 12.** Catalytic degradation mechanism (Hydrolysis and oxidative) pathways for
 838 selected CWAs.⁸ Reproduced from Ref. 8 with permission, Creative Commons Attribution
 839 3.0 Unposted License Copyright © 2014 Royal Society of Chemistry.

840

841
842

843 **Figure 13 (A & B)** Schismatic representation of Organic Photocatalysis through doped
 844 MOFs for Water Oxidation, Carbon Dioxide Reduction, (B) doped $[\text{Zr}_6\text{O}_4(\text{OH})_4(\text{bpdc})_6]$
 845 (UiO-67) systems and the resulting aerobic catalytic oxidation of thioanisole.¹⁰⁶ Reproduced
 846 from Ref. 106 with permission, Copyright © 2011, American Chemical Society.
 847

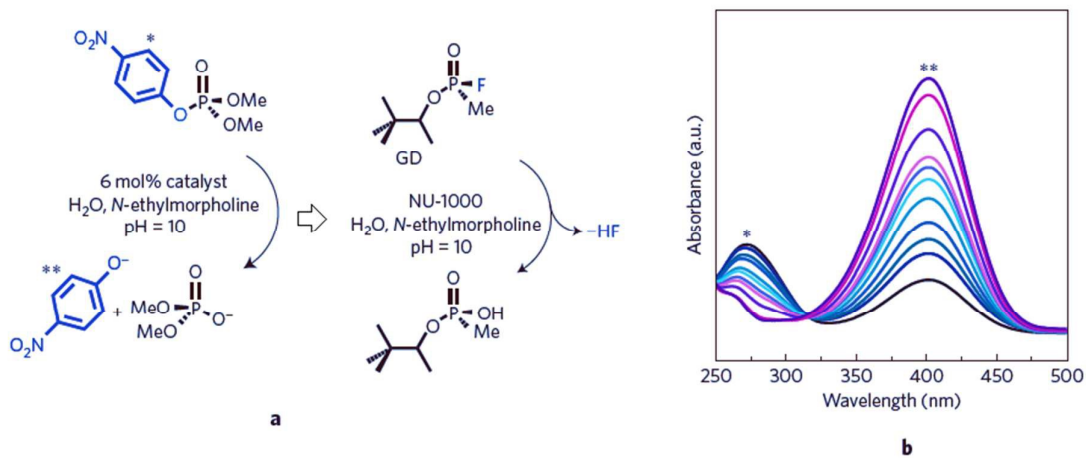


848

849

850 **Figure 14. (A & B) (A)** Hydrolysis mechanism of CWAs through utilization of MOFs **(B)**
851 UV-Vis spectra showing the formation of p-nitrophenoxide via visible-region adsorbance
852 spectroscopy at $E_{max} = 407$.¹¹⁰ Reproduced from Ref. 110 with permission, Copyright ©
853 2015, Nature Publishing Group.

854



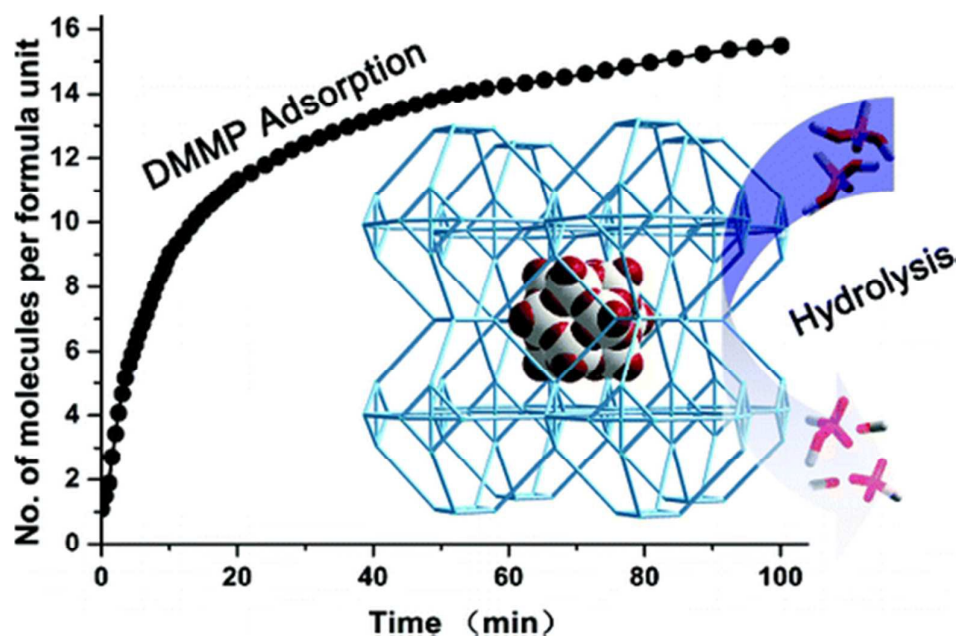
855

856

857 **Figure 15.** Schematic representation of Sodalite-type porous metal–organic framework with
858 polyoxometalate templates: adsorption and decomposition of dimethyl methylphosphonate.¹¹³

859 Reproduced from Ref. 113 with permission, Copyright © 2011, American Chemical Society.

860



861

862

863

864

Tables

Table 1. A list of conventional materials with respect to their CO₂ adsorption capacities.

Order	Conventional materials	Name	Experimental conditions Temp. (K) / CO ₂ partial pressure (bar)	CO ₂ adsorption capacity (mmol g ⁻¹)	Analytical Method	Reference
1	Activated Carbon	GAC ^a	298/0.1	0.057	Gas chromatography	53
2	Calcium oxides	CaO and Rb/CaO	723/0.4	4.5	Thermogravimetric analysis	54-55
3	Zeolites	APG-11 ^b	393/0.15 (Humid)	0.38	Mass spectrometer	56
4	Silica	SBA-15 ^c	333/0.15	0.03	Gas chromatography	57
5	Lithium Zirconates	Li ₂ ZrO ₃	773/0.02	4.5	Thermogravimetric analysis	58
6	Organic Hybrid Adsorbents	DETA ^d	298/1	0.91	Thermogravimetric analysis	59

^aGAC = Granular Activated Carbon,^bSBA-15 = Aminosilane-modified Zeolite^cAPG -11 = Na [(AlO) (SiO₂)]-xH₂O,^dDETA = Diethylenetriamine

Table 2. MOFs used as sorptive media for the treatment of airborne pollutants.**A. Major targets: CO₂, O₂, CH₃, and NH₃**

Sr. No.	MOF	Mechanism	Synthesis	Performance/ Capacity (mmol g ⁻¹)	Experimental conditions (Temperature /Pressure)	Reference
1	Mg-MOF-74	Metal Substitution	Solvothermal	8	296K at 1 bar	72
2	JUC-124	π - π stacking	Hydrothermal	2.72 & 1.71	273+293K at 1 bar	72
3	Co-MOF-74	Weak physisorption interactions	Solvothermal	5.66	298K at 1 bar	74
4	MOF-5	Postsynthesis thermal annealing	Solvothermal	2	293 K at 1 bar	75
5	MIL- 53 (Al)	CO ₂	Pressure swing adsorbation (PSA) process	4.3	303 K at 3.5 bar	76
6	EN-Mg ₂ (dobpdc)	Weak physisorption interactions	Hydrothermal	4.57 (16.7 wt%), 3.00 (11.7 wt%)	298+423 K at 1 bar	77
7	Amine- Mg(DOBDC) MOF	Weak physisorption interactions	Hydrothermal	9.09	-	78
8	QI-Cu-MOF	Hydrophobic Interaction	Solvothermal	4.56	293 K at 1 bar	79
9	NOTT-101	Hydrophobic	Solvothermal	3.93	293 K at 1 bar	80

10	M(dobpdc) (M = Mg, Mn, Fe, Co, Zn) Diamine-appended MOF/PCP	Interaction Thermodynamically non-spontaneous reaction (low P)	Solvothermal	2.2–2.3 MJ per kg (regeneration energies of Mg ₂ (dobpdc) and mmen-Mn ₂ (dobpdc) for CO ₂ captured)	-	81
11	{Zn(bpydb)(bpy)} _n (amino- and pyridine-functionalized pores)	Mixed-ligand strategy	Hydrothermal	3.6	273K at 1 bar	82
B. MOF for CH₄ treatment						
12	IRMOFs series (1-16)	Weak physisorption interactions	Solvothermal	240 cm ³ /g at standard temperature and pressure	298 K and 3.6 atm	83
13	IRMOF-1 and IRMOF-6	π - π stacking/interaction	Solvothermal	217.45 and 208.39 cm ³ (STP)/g	273K at 3.5 bar	84
C. MOF for NH₃ treatment						
14	Cu-MOF/GO		Solvothermal	8 m	-	88
15	HKUST-1		Solvothermal	6.8	348K at 1 bar	89
16	IRMOF-3	Electrostatic interaction	Solvothermal	6.2	293K at 1 bar	90
17	MOF-5		Solvothermal	0.35		91
18	MOF-5 and MOF-177	Electrostatic interaction	Hydrothermal	12.2	-	92
19	DUT-6	Hydrogen	Hydrothermal	13.6	273 K	93

		bonding interaction			at 1 bar	
20	Zr-based MOFs		Hydrothermal	5.7		94
21	IRMOF-8		Hydrothermal	16.4	298K at 1 bar	97
D. MOF for O₂ treatment						
22	Cu-BTC		Hydrothermal		77 K, 273–298 K	97
23	(Cr ₂ (BTC) ₃)	Unsaturated metal centers based mechanism	Hydrothermal		273K at 1 bar	98
24	Fe ₂ (DOBDC))		Hydrothermal		273K at 1 bar	98
25	FIR-51	Light hydrocarbons	Acid-base interactions	3.12 - 7.06	273 K at 1 bar	99
E. MOF for other targets by Hydrothermal synthesis						
26	MIL-101-Cr	Anionic dye or Methyl orange	Electrostatic interaction	2.59	273K at 1bar	100
27	ED-MIL-101-Cr and PED-MIL-101-Cr	Anionic dye or Methyl orange		3.86 and 4.40	273K at 1bar	101

28	NH ₂ -MIL-101-Al	Methyl blue and orange	Electrostatic interaction	17.31 and 4.27	-	102
29	MOF-235	Anionic dye or Methyl orange		10.84 and 4.25	-	103
30	Cu-BTC	Quantum chemical methods	Solvothermal	-82.32 kJ/mol	-	104
31	Cu-BTC		Solvothermal	-81.48 kJ/mol		105
32	Metal catecholate (Be-, Cu-, Zn-, Pt-, and Pd-catecholates) Based MOFs		Solvothermal	2.10 and 1.36 mmol/g	-	109
F. MOF for other targets by solvothermal method						
33	MIL-101-Cr and ZIF-8	Uranine	Electrostatic interaction	2.86 and 2.27	-	116
34	MIL-101-Cr	Xylenol orange	Electrostatic interaction	7.06	-	117
35	NH ₂ -UIO-66	NH ₃ , H ₂ S, and arsine	Hydrogen bonding	1.13-2.27	353 K at 1 bar	118
36	Cu-BTC	Pyridine	π - π stacking/interaction	7.8 (Dry) and 7.7 (Humid)	373K at 1 bar	119

Table 3. Functionalized MOFs utilized for catalytic treatment media of airborne pollutants

Sr. No.	Target Pollutants	CP/MOFs	Active metal ions	Catalytic mechanism/ strategies	Reference
A. Solvothermal synthesis					
1	CO ₂ and Thioanisole	UiO-67	Ir, Re, and Ru	Photocatalytic reduction	106
2	Alcohols	UiO-66(NH ₂)	Zr	Visible-light-driven photocatalysis	107
3	Methylene blue	MIL-53(Fe)	Fe	UV-vis light irradiation	108
4	DMNP and Soman	NU-1000		Hydrogenous catalyst	109
		NU-1000-dehyd (Zr-MOFs)	Zr		
5	VX and soman	HKUST-1	Zr, Cu	Hydrolysis process	110
B. Hydrothermal synthesis					
6	DIFP and DFP	NH ₂ - MIL-101(Al)	Fe, Al	Hydrogenous degradation	111
7.	DMMP	NH ₂ -MIL-53(Al) and NENU-11	Cu	Hydrolytic degradation	112
8	DMMP	NH ₂ -MIL-53(Al)	Fe	Hydrogenous catalyst	113
9	Aldehyde acetalization with ethanol	CHS@MOF	Cu	Self-template strategy	114

Metal organic frameworks for the control and management of air quality: Advances and future direction

Pawan Kumar¹, Ki-Hyun Kim^{1,*}, Eilhann E. Kwon², Jan Szulejko¹

¹Dept. of Civil & Environmental Engineering, Hanyang University, 222 Wangsimni-Ro, Seoul 133-791, Republic of Korea,

²Department of Environment and Energy, Sejong University, Seoul 143-747, Republic of Korea

*E-mail: kkim61@hanyang.ac.kr, Tel.: +82 2220 2325; Fax: +82 2 2220 1945

